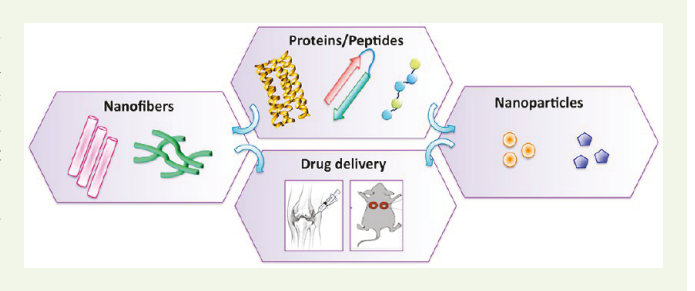


## Self-Assembled Protein- and Peptide-Based Nanomaterials

Priya Katyal, Michael Meleties, and Jin K. Montclare\*, , , , , , , , , , , , , , ,

ABSTRACT: Considerable effort has been devoted to generating novel protein- and peptide-based nanomaterials with their applications in a wide range of fields. Specifically, the unique property of proteins to self-assemble has been utilized to create a variety of nanoassemblies, which offer significant possibilities for next-generation biomaterials. In this minireview, we describe self-assembled protein- and peptide-based nanomaterials with focus on nanofibers and nanoparticles. Their applications in delivering therapeutic drugs and genes are discussed.



KEYWORDS: nanomaterials, protein engineering, self-assembly, protein-based micelles, protein-based fibers, drug delivery

### 1. INTRODUCTION

There has been a surge of nanomaterials comprising designer proteins and peptides with defined structures and functions because of recent developments in chemical and synthetic biology. Using proteins as building blocks, it is now possible to create nanoscale architectures ranging from few nanometers to hundreds of nanometers.<sup>2</sup> The unique properties of proteins including their modular nature, biocompatibility, and biodegradability offer exciting opportunities in designing smart nanomaterials.<sup>3,4</sup> Unlike synthetic polymers that are characterized by structural inhomogeneities and non-uniform chain lengths/molecular weight distribution, proteins are uniform in peptide length and molecular weight, resulting in biomaterials that are more precise in sequence, structure, and overall assemblies.

Protein- and peptide-based nanomaterials have been used for a myriad of biological applications, leveraging in large part their property to self-assemble. Inspired by nature, several proteins/peptides have been engineered to self-assemble into a variety of complex structures, ranging from nanoparticles, vesicles, cages and fibrous assemblies; these can be endowed with novel functionalities offering numerous applications in diverse areas of bioengineering.<sup>2,7–9</sup> Such proteins/peptides can be tailored with stimuli-responsive triggers that respond under specific conditions, thus providing a handle to control and customize the assembly and disassembly of nanomaterials.<sup>10</sup> Significant progress has been made in this area with the design of new structures that respond to various stimuli including pH, temperature, and ionic strength. 10,11

Several reviews have summarized the rationale, design, and applications of various nanoparticle assemblies. 1-4,8,12 Here, in this minireview, we focus on two self-assembling protein or peptide architectures: (1) fibers and (2) nanoparticles. The use

of these assemblies for drug delivery applications is discussed (Figure 1). The examples described herein are based on de novo peptides and recombinant proteins.

### 2. SELF-ASSEMBLED NANOFIBERS

2.1. Coiled-Coil-Based Nanofibers. Self-assembling proteins and peptides have been utilized as scaffolds to generate nanofibers. 13 The morphology and material properties of these nanofibers can be modulated through various strategies. Although there are a variety of secondary structural motifs employed in designing fibers, <sup>13–15</sup> in this section, we focus on coiled-coil based nanofibers. For example, Kojima et al. have developed short  $\alpha$ 3-peptides that form a homotetramer, which further assembles to form fibers 5-10 nm in diameter with visible protofibrils (Figure 2a, c, Table 1). At high salt concentrations, these protofibrils bundle together to form larger fibers (Figure 2d). When the sequence of the  $\alpha$ 3-peptide is reversed to generate r3-peptide, much longer fibers having a similar diameter are obtained (Figure 2b, e, Table 1).<sup>17</sup> These fibers are further stabilized under the conditions of high salt and neutral pH (Figure 2f).17

Alternatively, Woolfson and co-workers used two 28 residue long self-assembling peptides, which when mixed form stickyend heterodimers, resulting in fibers with diameters of about 20 nm as depicted by transmission electron microscopy (TEM) (Figure 3). The peptides SAF-p1 and SAF-p2 (Table 1), derived from leucine zipper-like motifs, comprise of typical heptad repeating units designated as *abcdefg*. <sup>18,19</sup> These

Received: March 23, 2019 Accepted: July 12, 2019 Published: July 12, 2019

<sup>&</sup>lt;sup>†</sup>Department of Chemical and Biomolecular Engineering, Tandon School of Engineering, New York University, Brooklyn, New York 11201, United States

<sup>&</sup>lt;sup>‡</sup>Department of Radiology, New York University Langone Health, New York, New York 10016, United States

Department of Biomaterials, College of Dentistry, New York University, New York, New York 10010, United States

Department of Chemistry, New York University, New York, New York 10003, United States

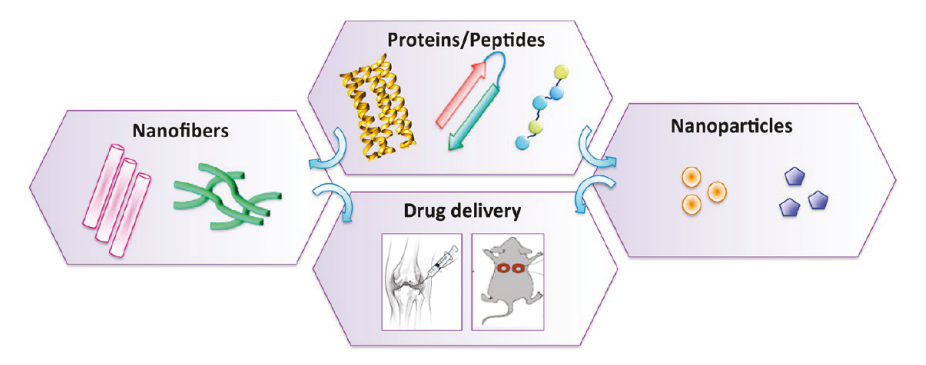
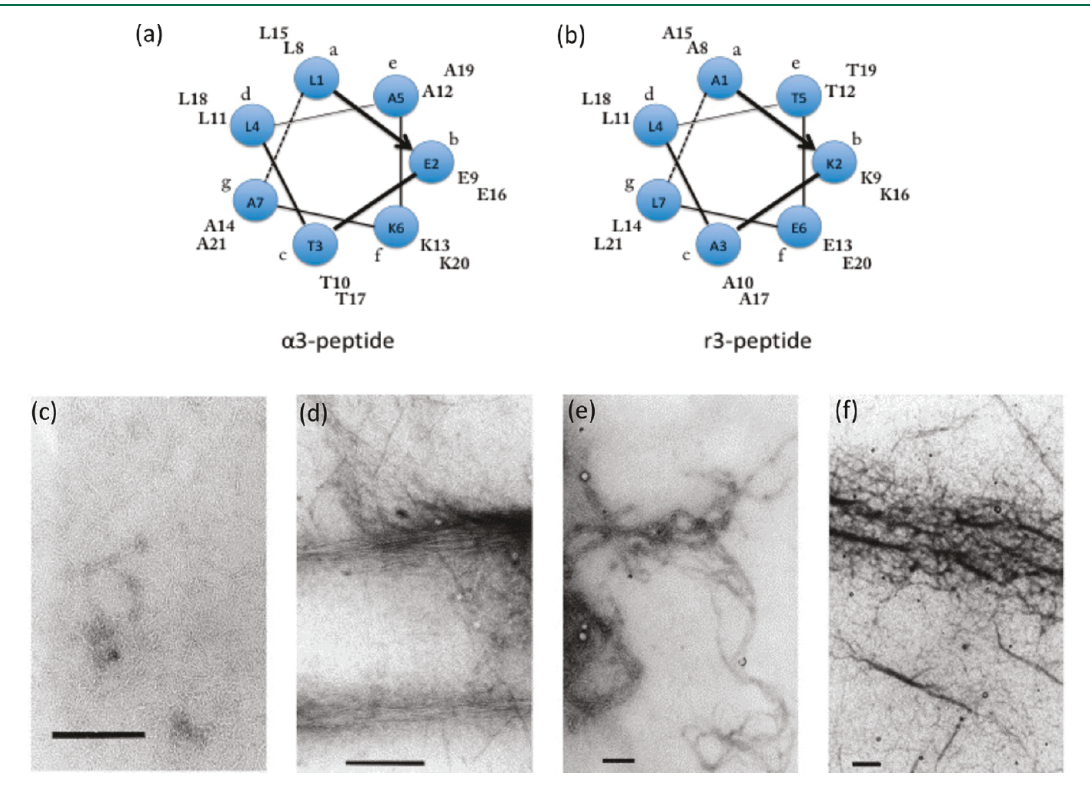


Figure 1. Schematic representation of protein- and peptide-based self-assembled nanofibers and nanoparticles and their applications in drug delivery.



**Figure 2.** Helical wheel representation of (a)  $\alpha$ 3-peptide and (b) r3-peptide. Electron micrographs of the  $\alpha$ 3-peptide in 10 mM phosphate (pH 6.0) containing (c) 0.1 M KCl or (d) 1.0 M KCl and the r3-peptide in 10 mM phosphate (pH 6.0) containing (e) 0.1 M KCl or (f) 1.0 M KCl. The scale bar represents (a-c) 250 nm and (d) 500 nm. Adapted with permission from ref 17. Copyright 2005 Elsevier.

peptides have isoleucine and leucine at a and d positions, respectively that promote coiled-coil dimerization. In addition, SAF-p1 and SAF-p2 include charged glutamic acid and lysine residues at positions e and g, resulting in complementary "stickyends" assembly. Another peptide SAF-p3 (Table 1), engineered by swapping regions of SAF-p1, results in blunt-ended heterodimers after mixing with SAF-p2. In contrast to sticky-ends dimers, these blunt-dimers do not result in fibril formation. <sup>18</sup>

The Montclare group explored the coiled-coil domain of cartilage oligomeric matrix protein (COMPcc), a non-collagenous extracellular matrix protein, comprising of five identical  $\alpha$ -helices and a central hydrophobic pore to which small hydrophobic molecules such as curcumin, vitamin D, and all-trans-retinol can bind. <sup>20–22</sup> A serine variant of COMPcc, COMPcc<sup>s</sup>, or His<sub>6</sub>-C, has been shown to self-assemble into nanofibers in the range of 10–15 nm (Figure 4a, Table 1). <sup>23,24</sup> This ability to self-assemble into fibers renders COMPcc<sup>s</sup> an interesting candidate for further research. By using single alanine mutagenesis, Gunasekar et al. have delineated the

residues important for COMPcc<sup>s</sup> to form a coiled-coil fiber.<sup>23</sup> Two variants of COMPcc<sup>s</sup>, His<sub>6</sub>-T40A and His<sub>6</sub>-L44A have been studied. While His<sub>6</sub>-T40A maintains its ability to form fibers, His<sub>6</sub>-L44A exhibits a loss in helical content, indicating that leucine is critical for fiber formation (Figure 4b, c, Table 1). The overall results of the study show that the hydrophobic residues are important for COMPcc<sup>s</sup> to self-assemble into nanofibers.<sup>23</sup>

Another method to create self-assembled fibers with defined properties involves 3D domain swapping of the proteins. <sup>25</sup> The mechanism of domain swapping involves the exchange of structural elements within a protein or between different proteins to form stable oligomers. <sup>26</sup> Of particular importance is the work by Ogihara et al., pertaining to domain swapped 3-helix bundles resulting in fibrils ranging from 40 to 70 nm in diameter. <sup>25</sup> They have redesigned a triple-helix bundle by swapping portions of  $\alpha$ -helical subunits with the deletion of a hairpin loop. The resulting variants differ in the orientation of helix III with respect to helix I (Figure 5). The monomer where helix III is parallel to helix I result in domain-swapped

Table 1. Sequences of Peptides/Proteins That Self-Assemble into Fibers

nomenclature	sequence	re
α3-peptide	(LGTLALA) <sub>3</sub>	16
r3peptide	(ALALTGL) <sub>3</sub>	17
SAF-p1	KIAALKQKIASLKQEIDALEYENDALEQ	18
SAF-p2	KIRALKAKNAHLKQEIAALEQEIAALEQ	18
SAF-p3	EIDALEYENDALEQKIAALKQKIASLKQ	18
COMPcc <sup>s</sup> (His <sub>6</sub> -C)	MRGSHHHHHHGSGDLAPQMLRELQETNAALQDVRELLRQQVKEITFLKNTV MESDASGKLN	23
His <sub>6</sub> -T40A	$MRGSHHHHHHGSGDLAPQMLRELQE \underline{\textbf{A}}\textbf{N} \textbf{A}\textbf{A}\textbf{L} QD\textbf{V} \textbf{R}\textbf{E}\textbf{L}\textbf{R}Q\textbf{V} \textbf{K}\textbf{E}\textbf{I}\textbf{T}\textbf{F}\textbf{L}\textbf{K}\textbf{N}\textbf{T}\textbf{V} \ \textbf{M}\textbf{E}\textbf{S}\textbf{D}\textbf{A}\textbf{S}\textbf{G}\textbf{K}\textbf{L}\textbf{N}$	23
His <sub>6</sub> -L44A	$MRGSHHHHHHGSGDLAPQMLRELQETNAA \underline{A}QDVRELLRQQVKEITFLKNTVMESDASGKLN$	23
Q	MRGSHHHHHHGSIEGRVKEITFLKNTAPQMLRELQETNAALQDVREL	27
CC-Di	Ac-GEIAALKQE IAALKKE NAALKWE IAALKQ GYY-NH $_{\mathrm{2}}$	28
CC-Tri	Ac-GEIAAIKQE IAAIKWE IAAIKQ GYG -NH $_{\mathrm{2}}$	28
CC-Tet	Ac-GELAAIKQE LAAIKKE LAAIKWE LAAIKQ GAG $-$ NH $_2$	28
CC-Tet2	Ac- GNILQE VKNILKE VKNILWE VKNILQE VK ${\rm G}$ -NH $_2$	28
CC-Pent	Ac-GKIEQI LQKIEKI LQKIEWI LQKIEQI LQ G -NH2	28
CC-Hex	Ac-GELKAIAQE LKAIAKE LKAIAWE LKAIAQ GAG -NH $_{\mathrm{2}}$	28
CC-Hex2	Ac-GEIAKS LKEIAWS LKEIAKS LK G -NH $_{\mathrm{2}}$	28
CC-Hex3	Ac-GEIAQS IKEIAKS IKEIAWS IKEIAQS IK G -NH $_{ m 2}$	28
СС-Нер-Т	Ac-GEIAQA LKEIAKA LKEIAWA LKEIAQA LK G -NH $_{ m 2}$	28
FF dipeptide	NH <sub>2</sub> -FF-COOH	30
CPII	$(PRG)_4(POG)_4(EOG)_4$ (O = hydroxyproline)	37
non-ionic peptides	$O_n(SL)_6O_n$ $(n = 1 - 6)$ $(O = hydroxyproline)$	39

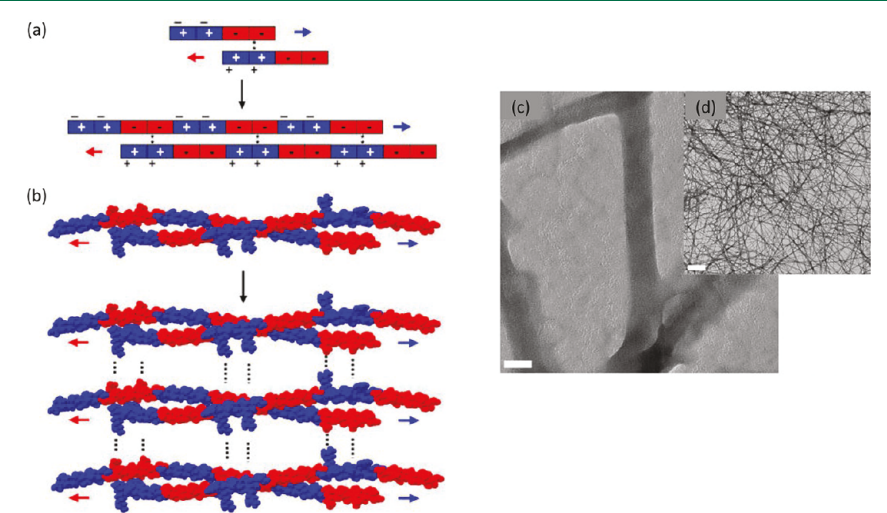
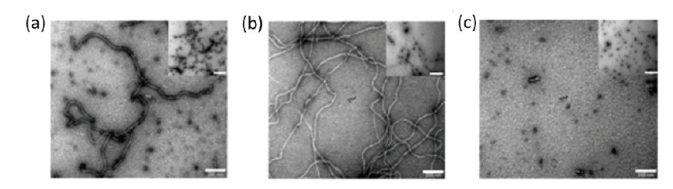


Figure 3. Self-assembling fibers based on "sticky-ends" peptides. The complementary charged residues on the pair of peptides result in (a) formation of staggered heterodimers, and (b) elongation and thickening of fibrils. (c, d) Electron micrographs of fibrils assembled upon mixing SAF-p1 with SAF-p2. Scale bars in c and d represent 50 nm and 2  $\mu$ m. Adapted with permission from ref 19. Copyright 2007 National Academy of Sciences.



**Figure 4.** TEM images of (a) His<sub>6</sub>-C, (b) His<sub>6</sub>-T40A, and (c) His<sub>6</sub>-L40A. Scale bar represents 200 nm and 1  $\mu$ m in the insets. Adapted with permission from ref 23. Copyright 2012 Wiley-VCH Verlag GmbH & Co.

dimers (DSD) (Figure 5a), whereas when the helices are antiparallel to each other, the C-terminal domain is always free to interact with other chains to create fibers comprising of bundles of protofibrils (Figure 5b, c).<sup>25</sup>

A variation of domain swapping has been used by Hume et al. to generate Q.<sup>27</sup> The deletion of the last heptad repeat (VMESDAS) of COMPcc<sup>s</sup>, along with swapping of the N- and C-terminal residues results in optimal surface charge distribution with Q demonstrating patches of positively and negatively charged surface residues (Figure 6a, Table 1). This allows lateral fiber assembly with Q organizing into nanofibers ranging from 20 to 560 nm under acidic pH conditions. Furthermore, Q self-assembles into robust nano- to mesoscaled fibers that is dependent on binding to a small molecule, curcumin (Figure 6b).<sup>27</sup>

Hollow (nanotubes) and solid nanofibers can also be synthesized by employing peptides derived from alternative coiled-coil (CC) sequences (Figure 7, Table 1).<sup>28</sup> A range of peptides with different oligomerization states (named as CC-trimer

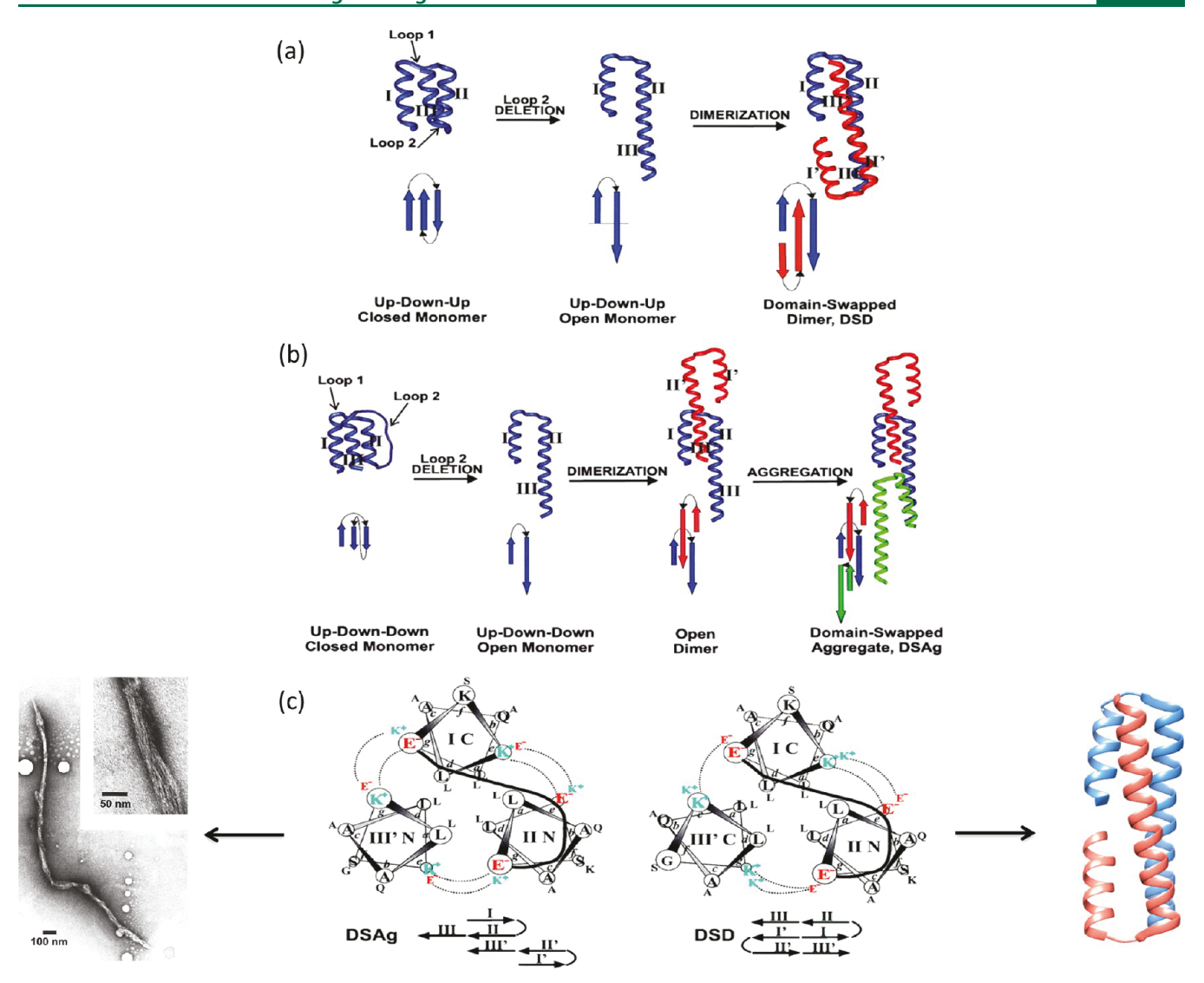


Figure 5. Design of (a) domain-swapped dimer (DSD) and (b) domain-swapped aggregate (DSAg). (c) Helical wheel representation of DSAg and DSD. DSAg self-assembles to form fibers composing of several protofibrils (inset), whereas DSD forms a dimer (pdb id:1G6U). Adapted with permission from ref 25. Copyright 2001 National Academy of Sciences.

through CC-heptamer), designed to promote end-to-end association, assemble into fibrous structures. Among the different constructs, thermal annealing of CC-Hex-T fibers results in highly ordered nanotubes (Figure 7d). Because of their hollow nature, the lumen of the nanotubes is accessible to bind to small molecules. Subsequently, these nanotubes have been shown to encapsulate a hydrophobic dye 1,6-diphenylhexatriene (DPH) exhibiting their potential as drug delivery vehicles.<sup>28</sup>

# **2.2.** Nanofibers Based on Other Structural Motifs. Analogous to coiled-coils, other specialized structural motifs like diphenylalanine (FF) and collagen mimetic peptides (CMPs), can also self-assemble to form nanofibers and nanotubes. The FF dipeptide, representing the core recognition motif of the $A\beta$ -amyloid peptides, is a short motif that can self-assemble into hollow nano- and microscale tubes (Figure 8, Table 1). <sup>29,30</sup> The assembly of such microtubes is multifaceted, with the first step being the formation of cyclic FF hexamers by six FF units. The hexamers then stack to form narrow channels, which subsequently produce sheets. The coiling of these sheets form nanotubes with the

hydrophobic/hydrophilic internal walls and hydrophobic external walls. These nanotubes then bundle together to form hollow microtubes (FF-MTs) (Figure 8).<sup>30</sup> Silva et al. have evaluated the ability of these systems as drug delivery vehicles, where they utilize FF-MTs to transport polar molecules, using Rhodamine B (RhB) as a model drug.<sup>30</sup> Furthermore, several strategies have been employed to modify FF dipeptides, which instead of forming nanotubes, result in nanofiber assembly.<sup>31,32</sup> These nanofibers have been used as carriers for hydrophobic drug molecules such as 10-hydroxycamptothecin with potential applications in cancer therapy.<sup>32</sup>

Collagen mimetic peptides (CMPs), on the other hand, comprise of glycine (G)- and proline (P)-rich sequence repeats (X-Y-G)<sub>n</sub>, where X and Y are proline and (4R)-hydroxyproline (O), respectively.<sup>33</sup> Several groups have studied X-Y-Glybearing peptides that fold to form triple-helix-based fibrils, a structural feature unique to collagen.<sup>34–36</sup> Work by Conticello and Chaikof has garnered significant attention in the field, as they were the first to report the CMP-based fibers exhibiting D-periodicity of collagen, another hallmark feature of collagen fibril.<sup>37</sup> The CMP, referred as CPII, consists of

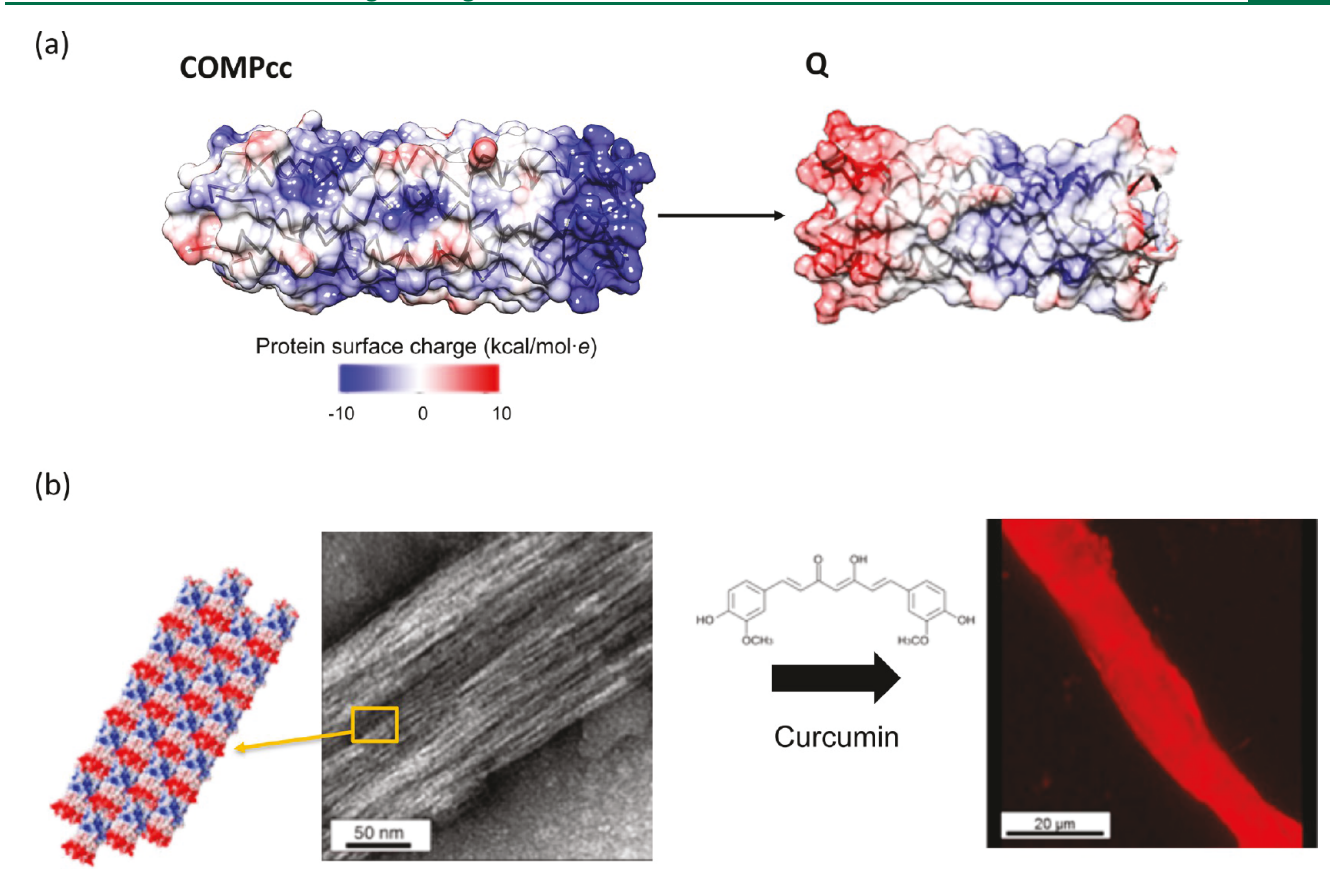


Figure 6. (a) Surface charge representation of COMPcc and Q proteins. (b) Self-assembly of Q nanofibers, which upon curcumin binding form mesoscale fibers. Panel b adapted with permission from ref 27. Copyright 2014 American Chemical Society.

three different sets of X-Y-G motif bearing a central core of P-O-G flanked by a positively charged domain at the N-terminus and a negatively charged domain at the C-terminus (Figure 9a, Table 1). Thermal annealing of CPII results in nanofibrils, which upon incubation at room temperature for 9 days, lead to formation of micron scaled fibers with D-periodic spacing (Figure 9b). These microfibers self-assemble via end-to-end and lateral associations mediated by hydrophobic interactions between the central domain and strong electrostatic interactions between arginine-glutamate residues present on adjacent fibrils, respectively (Figure 9c).<sup>37</sup> Hartgerink and colleagues have replaced the arginine-glutamate interactions in the abovementioned CMP with a lysine-aspartate pair, which resulted in effective fiber assembly. These nanofibers pack together to form a hydrogel that has a degradation profile similar to rat-tail collagen.<sup>38</sup>

In addition to CMPs, the Hartgerink group has also prepared a neutral nanofiber hydrogel by utilizing hydroxyproline (O) bearing nonionic peptides (Table 1). The design of the peptide includes an amphiphilic core comprising of (SL)<sub>6</sub> that is capable of adopting  $\beta$ -sheet conformation and can assemble into nanofibers. The N- and C-termini of the peptide comprise of repeats of neutral hydroxyproline domains, which can form polyproline type II helices (Figure 10). TEM analysis of the resulting peptide series,  $O_n(SL)_6O_n$ , reveals an increase in the length of nanofibers with a higher number of hydroxyproline residues. An increase in PPII content is suggested to be responsible for creating molecular and steric frustrations, thereby affecting the peptide solubility and nanofibers structure. Interestingly, only  $O_5(SL)_6O_5$  exhibits an optimized balance of solubility, rigidity, and fiber length that resulted in hydrogel

assembly under all the pH conditions tested. Further cell-based studies show potential biomedical applications of such neutral biocompatible fibrous systems.<sup>39</sup>

### 3. SELF-ASSEMBLED NANOPARTICLES

In the context of this minireview, protein engineered nanoparticles differ from protein fibers in the mode of self-assembly. Whereas protein fibers will assemble into filamentous structures, the term nanoparticle is used to refer to protein complexes that are more spherical, including micelles. Although fiber assembly has been dominated by protein and peptides with a single conformation, 16–18,23,27,28 in the following section, nanoparticle assemblies rely on the stitching of two domains that can comprise single or multiple conformations.

**3.1. Self-Assembled Amphiphilic Micelles.** Protein engineering can be utilized to develop new protein-based assemblies and related biomaterials. One such example includes the design and use of protein-based block polymers. These polymers are made up of two or more distinct protein sequences, or "blocks" that can be fused together in different arrangements. Hybrid block polymers consisting of hydrophilic and hydrophobic domains are of particular interest for the construction of self-assembled nanomaterials. Because of their amphiphilic nature, these proteins can often pack into micelles, which typically consist of a hydrophobic inner core surrounded by the hydrophilic shell (corona).

The most widely used polypeptides for generating micelles are based on the elastomeric protein having a consensus sequence of (Val-Pro-Gly-X-Gly), where 'X' is an interchangeable

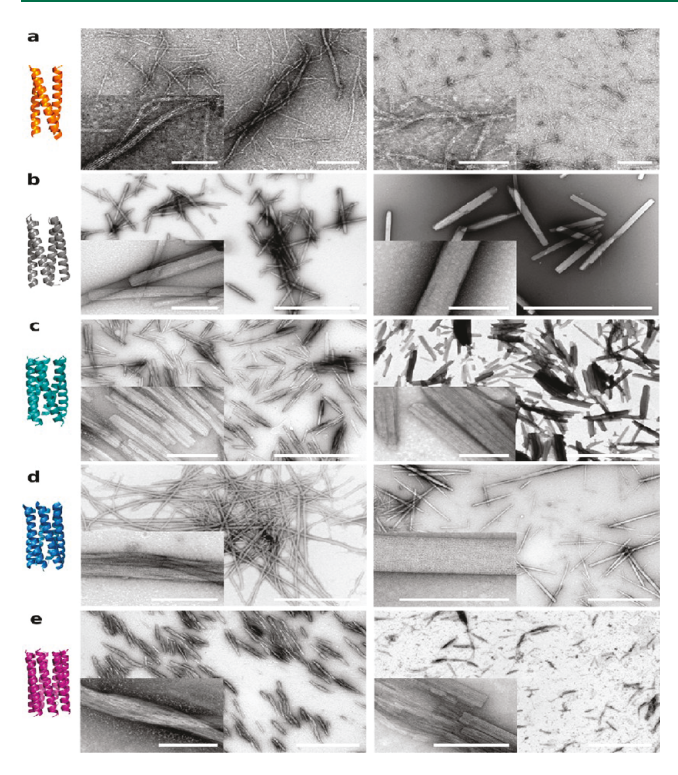


Figure 7. TEM images of solid nanofibers and nanotubes. (a) CC-Tri-F, (b) CC-Tet2-F (CC-Tet crystal structure shown in gray), (c) CC-Pent-T, (d) CC-Hex-T, and (e) CC-Hept-T. Scale bars: (a) 200 nm, inset = 100 nm; (b-e) 2000 nm, inset = 200 nm. Left: X-ray crystal structures (available for all but CC-Tet2). Middle: Micrographs for samples prepared at 20 °C. Right: Images of fibers after their thermal annealing. F and T indicate that the oligomer would form fibers or nanotubes. Reproduced with permission from ref 28. Copyright 2015 American Chemical Society.

amino acid and 'n' is the number of repeats. 43 The hydrophobicity and mechanical properties of these peptides can be tuned by varying either X or n. These polypeptides, referred to as elastin-like polypeptides or ELPs, are characterized by their unique lower critical solution temperature (LCST or  $T_t$ ) transition. 44 At temperatures below their  $T_t$ , ELPs exist in solution, whereas at higher temperatures (beyond  $T_t$ ), they form insoluble coacervates or higher order aggregates. 45 ELPs with lower  $T_{\rm t}$  exhibit more hydrophobicity in contrast to polypeptides with higher  $T_t$ . Dreher et al. utilized this thermoresponsive property of ELPs to design a series of amphiphilic polymers. 46 These peptides comprise an N-terminal hydrophilic block of [V<sub>1</sub>A<sub>8</sub>G<sub>7</sub>-n] fused to a hydrophobic C-terminal block consisting of [V<sub>5</sub>-n] (Figure 11, Table 2). ELPs with different lengths and ratios of hydrophilic-to-hydrophobic block have been examined for their ability to form spherical micelles at the clinically relevant temperature range of 37-42 °C.46 A hydrophilic-to-hydrophobic ratio between 1:2 and 2:1 has been found to be ideal for micellar assembly with the size ranging from 29 to 39 nm. Furthermore, ELP constructs decorated with tumor targeting motifs self-assemble into micelles, enabling temperature triggered multivalent display of these ligands to tumor cells (Figure 11). Such micelles have tremendous potential in drug delivery and bioimaging applications. 46

Another strategy for generating self-assembled micelles relies on combining blocks of ELPs with other functional proteins. <sup>47,48</sup> Montclare and colleagues have synthesized a series of block

polymers comprising of COMPccs (C) and ELP (E). The designed diblock polymers,  $E_nC$  and  $CE_n$  (n = 1-5), assemble into particles with a diameter of 26-30 nm (Figure 12, Table 2). 49 The number of repeats of E (n) and orientation of the blocks control the conformation and mechanical properties, 50,51 with E,C polymers exhibiting more elastic character compared to the CE<sub>n</sub> library. 49 Similarly, triblock polymers such as ECE and CEC can self-assemble into nanoparticles with ECE demonstrating viscoelastic character and CEC showing elastic character (Figure 12, Table 2).51,52 Interestingly, appending an extra C domain to CE improves its structural, thermal, and mechanical properties. Recently, CEC has been reported to form hydrogels upon dynamic association of micellar assemblies.<sup>52</sup> The reported set of C- and E-bearing block polymers is capable of binding small molecules (for example, curcumin) and has great utility in increasing bioavailability of poorly water-soluble drugs.5

The elastin block polymers have also been combined with the silk domain to form micellar-like particles. 48 Kaplan and co-workers have constructed three silk-elastin-like protein polymers (SELPs), SE8Y, S2E8Y, S4E8Y (Figure 13a, Table 2), consisting of repeating units of silk (GAGAGS) and elastin (GXGVP). 48 Although the hydrophobic silk domains form the core structure of the micellar particles, the corona comprises hydrophilic elastin domains. The size of the particles is governed by the ratio of silk to elastin blocks; increasing the number of silk repeats increases the overall size of the particles. The assembly of these polymers are further controlled by their transition temperature. 48 Upon heating, SE8Y and S2E8Y particles coalesce to form larger-sized particles, whereas S4E8Y exhibits irreversible gel-like behavior (Figure 13b). Cooling the polymer solutions of SE8Y and S2E8Y back to 20 °C results in assemblies varying from nanoparticles to nanofibers and higherorder aggregates. 48 These polymers display great potential in encapsulating hydrophobic drugs and have been explored as potential drug delivery carriers for the treatment of cancer. 5

3.2. Self-Assembling Protein Nanoparticles (SAPN). In the pursuit of designing novel assemblies, the Burkhard group used computer modeling to build protein sequences that can assemble into nanoparticles with defined shape, size, and symmetry.<sup>54</sup> These self-assembling protein nanoparticles, or SAPNs, differ from micellar-based assemblies as they have polyhedral symmetry and are inspired from the symmetrical structure of viral capsids. 55 The rationally designed protein used for such assemblies comprise of two coiled-coil domains, a COMPcc pentameric unit and a de novo designed trimeric coiled-coil (derived from a leucine zipper), connected via glycine linker (Figure 14a, Table 2). Because the shape of these particles resembles that of viral capsids, they are capable of eliciting strong immune response. These engineered assemblies (Figure 14b) have been used as vaccine adjuvants and are utilized for multivalent display of epitopes. 56,57 Sequences of known pathogenic proteins (e.g., HIV surface protein gp41) are designed into the sequence of monomeric chain, which upon assembly display the antigens on the surface of the nanoparticles (Figure 14c).5

# 4. APPLICATIONS OF SELF-ASSEMBLED NANOMATERIALS

The concept of using protein- and peptide-based nanomaterials holds great promise for a variety of applications, particularly for biomedical fields. These nanomaterials are an ideal avenue for drug delivery not only because of their inherent

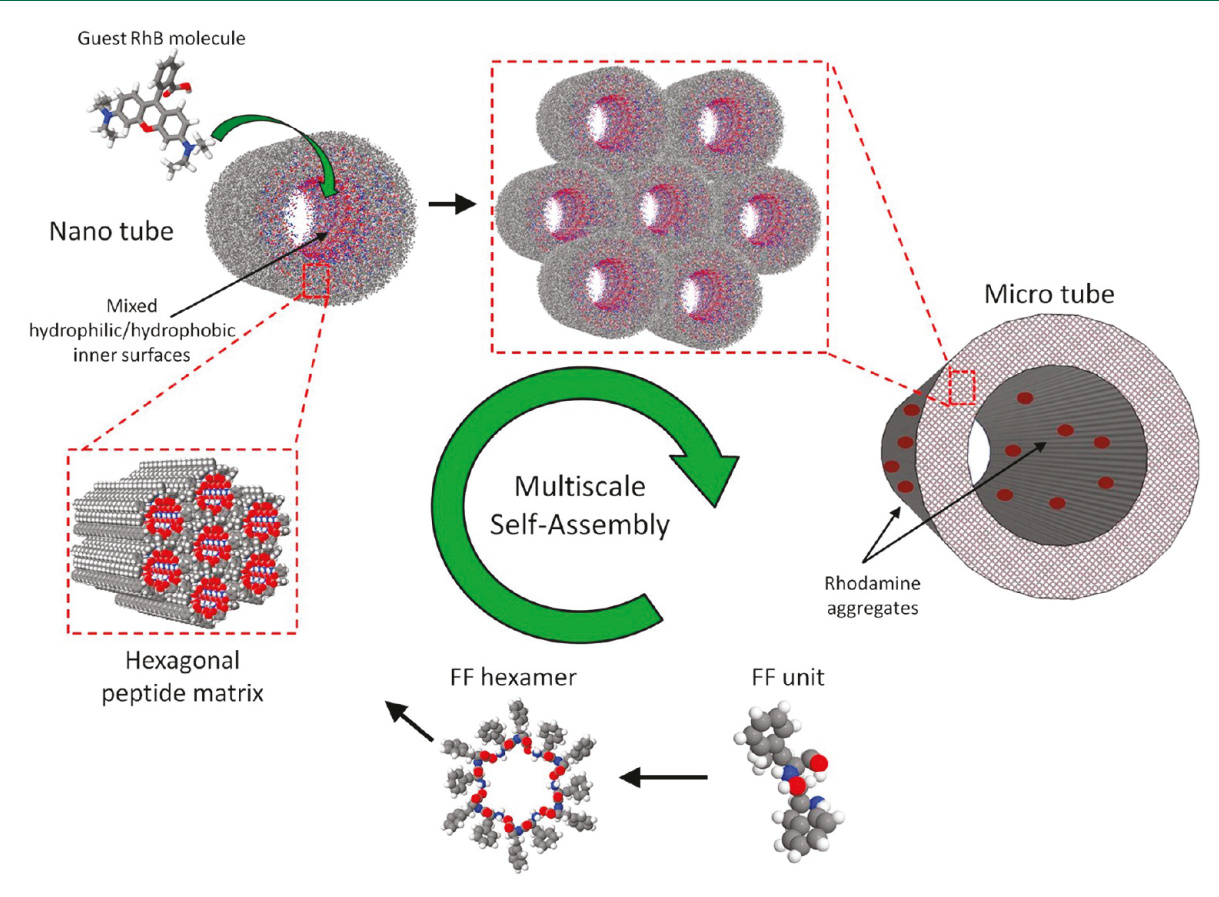


**Figure 8.** Schematic representation of FF microtubes assembly. Six units of FF dipeptide form an FF hexamer that packs together to form a hexagonal matrix. Further packing of these matrices results in nano- and microscale tubes capable of binding polar molecules like rhodamine B (RhB). Reproduced with permission from ref 30. Copyright 2013 American Chemical Society.

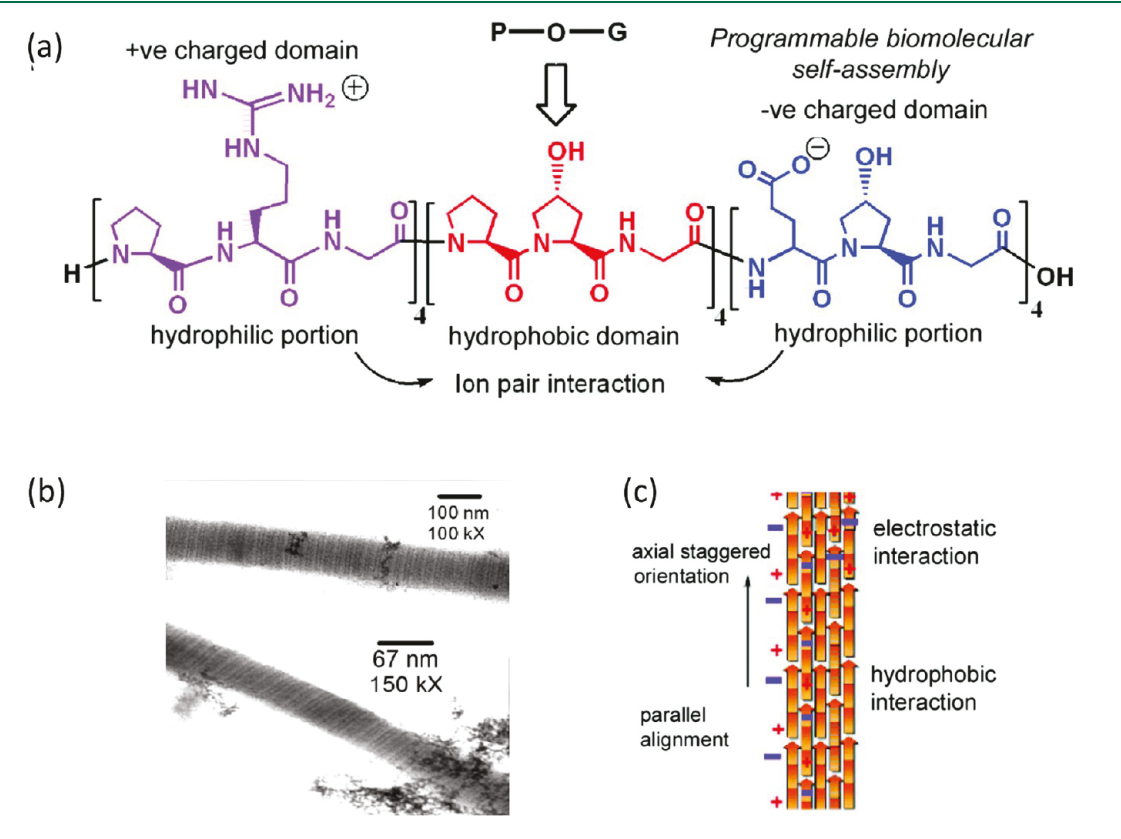


**Figure 9.** (a) Amino acid sequence of CPII with a central P-O-G domain. (b) TEM micrograph showing D-periodic microfibers. (c) Schematic representation of interactions important in CMP microfibers assembly. Adapted with permission from ref 37. Copyright 2007 American Chemical Society.

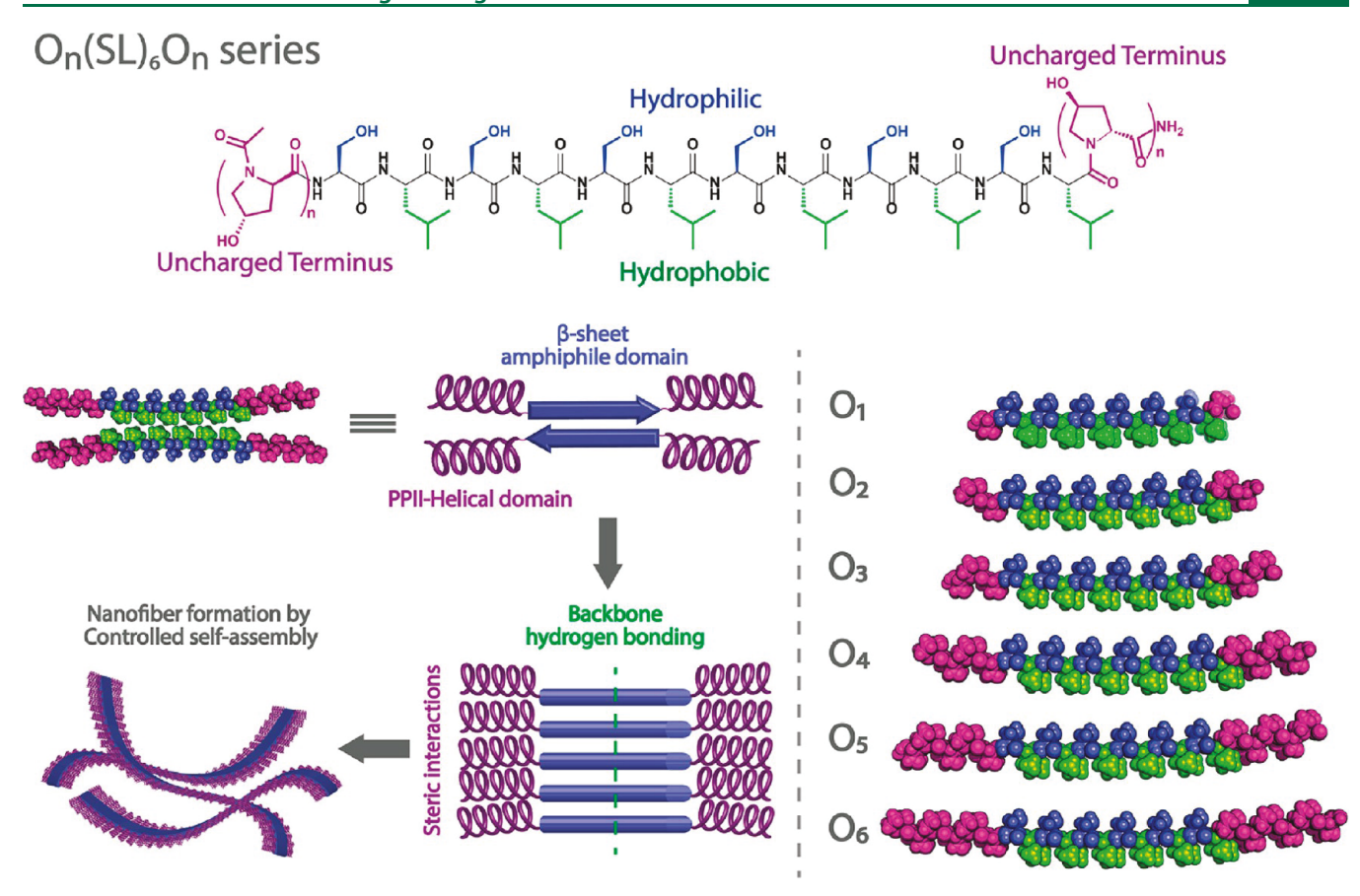
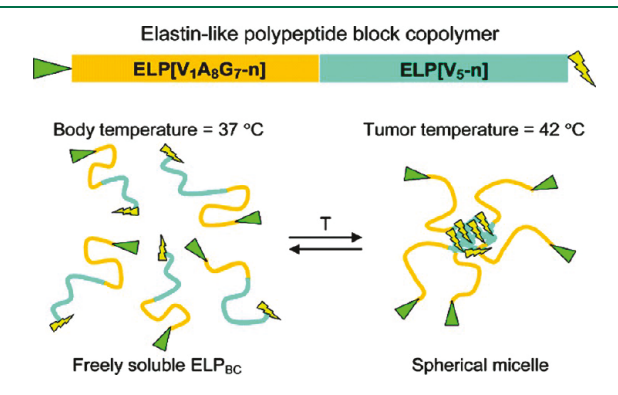


Figure 10. Design of hydroxyproline bearing non-ionic peptides,  $O_n(SL)_6O_n$ , where n varies from 1 to 6. The amphiphilic (SL)<sub>6</sub> domain self-assembles to form β-sheet conformation with hydroxyproline bearing motifs adopting PPII helical conformation at the N- and C-termini. Overall, these peptides self-assemble to form nanofibers. Reproduced with permission from ref 39. Copyright 2019 American Chemical Society.



**Figure 11.** Self-assembly of a thermoresponsive ELP block polymer forming spherical micelles. Upon self-assembly, these micelles display multiple copies of a tumor-targeting moiety (green triangle) and sequester a drug (lightning bolt) within the core of the micelle. Reproduced with permission from ref 46. Copyright 2008 American Chemical Society.

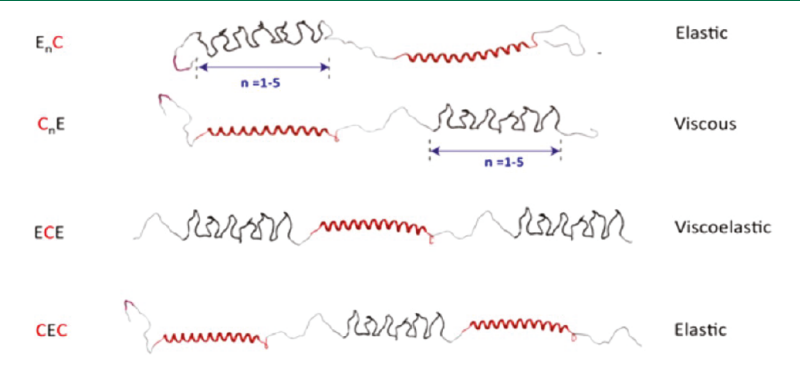
biodegradability and biocompatibility properties but also because these self-assembled structures can meet the general criteria considered for a successful drug delivery vehicle. They provide: (1) effective encapsulation of the drug; (2) the ability to transport the drug to a desired location; and (3) the capability to efficiently release the drug moiety in accordance with its desired application. <sup>64,65</sup>

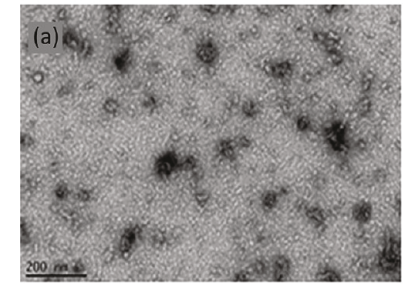
Coiled-coil-based protein fibers are especially prominent in the delivery of hydrophobic molecules. 66,67 These molecules normally suffer from an inherently low bioavailability stemming from their hydrophobicity. By using fibers, these hydrophobic small molecule therapeutics can be effectively housed and delivered to a desired site. Yin et al. employed protein nanofibers for the delivery of a potential osteoarthritic (OA) therapeutic that suffers from poor aqueous solubility.<sup>24</sup> Specifically, COMPcc<sup>5</sup> nanofibers on the order of 10 nm have been used to encapsulate and deliver BMS493 (((E))4-[2-[5,5-dimethyl-8-(2-phenylethynyl)-5,6-dihydronaphthalen-2-yl]ethen-1-yl]benzoic acid), providing a sustained release over a three day period in in vitro articular chondrocytes assay.<sup>24</sup> Because all-trans retinoic acid (ATRA) binds these nanofibers with higher affinity, it can trigger the release of BMS493 from COMPcc<sup>5</sup> fibers within the OA joints (Figure 15).<sup>24</sup>

Similar to fibers, micelles also have utility as cargo carriers, having been employed in a number of biomedical applications.  $^{68-70}$  Elastin-based micelles have been exploited for encapsulation of various chemotherapeutic agents, small hydrophobic molecules and other model drugs.  $^{71-73}$  In addition, these assemblies have been increasingly used for tumor targeting. The functionalization of these micelles with tumor targeting peptides enhances their ability to accumulate within the tumor.  $^{46,69}$  For example, injection of ELP-based micelles decorated with AP1 peptide result in their accumulation at the site of the tumor in breast cancer mice models. AP1 peptide binds selectively to interleukin-4 (IL-4) receptors that are overexpressed on a variety of tumors. Two elastin-based polymers,  $[\mathrm{V}_{14}]_6$  and  $[\mathrm{AP1-V}_{12}]_6$ , conjugated to a fluorophore have been imaged using live optical imaging system (Figure 16, Table 2). The AP1-bearing peptide reveals fluorescence at the

Table 2. Sequences of Peptides/Proteins That Self-Assemble into Nanoparticles

nomenclature	sequence	ref
ELP $[V_1A_8G_7-n]$	$MSKGPG [(VPGVG) (VPGAG)_8 (VPGGG)_7]_nYP$	46
ELP $[V_5-n]$	$MSKGPG [(VPGVG)]_nYP$	46
$E_nC$	$MRGSH_6GSKPIAASA$ - $E_n$ - $LEGSELA(AT)_6AACG$ - $C$ - $LQA(AT)_6AVDLQPS$	49
$C_nE$	$\label{eq:mrgsh_6} MRGSH_6GSACELA(AT)_6AACG-C-LQA(AT)_6AVDKPIAASA-E_n-LEGSGTGAKL$	49
ECE	$\label{eq:mrgsh_6} MRGSH_6GSKPIAASA-E_{s}\text{-}LEGSELA(AT)_6AACG-\textbf{C}\text{-}LQA(AT)_6AVDKPIAASA-\textbf{E}_{s}\text{-}LEGSGTGAKLN$	50
CEC	$\label{eq:mrgsh_gaacela} MRGSH_{6}GSACELA(AT)_{6}AAC\text{-}C\text{-}LQA(AT)_{6}AVDKPIAASA\text{-}E_{5}\text{-}LEGSGT\text{-}C\text{-}LQALSI$	52
E	$[(VPGVG)_2VPGFG(VPGVG)_2]_nVP$	49
С	GDLAPQMLRELQETNAALQDVRELLRQQVKEITFLKNTVMESDASG	49
SE8Y	$[(GAGAGS)(GVGVP)_{4}(GYGVP)(GVGVP)_{3}]$	48
S2E8Y	$[(GAGAGS)_2(GVGVP)_4(GYGVP)(GVGVP)_3]$	48
S4E8Y	$[(GAGAGS)_4(GVGVP)_4(GYGVP)(GVGVP)_3]$	48
SAPN (monomer)	${\tt AcDEMLRELQETNAALQDVRELLRQQVKQITFLKCLLMGGRLLCRLEELERRLEELERR-NH_2}$	55
$[V_{14}]_6$	$SGPG[(VPGVG)_{14}]_6WPC$	59
$[AP1-V_{12}]_6$	$SGPG[VGRKRLDRNG(VPGVG)_{12}]_6WPC$	59
SI	$G(VPGSG)_{48}(VPGIG)_{48}Y$	60
FSI	$FKBP-G(VPGSG)_{48}(VPGIG)_{48}Y$	60
	FKBP: MGVQVETISPGDGRTFPKRGQTCVVHYTGMLEDGKKFDSSRDRNKPFKFMLGKQEVIRGWEEGVAQMSVGQRAKLTISPDYAYGATGHPGIIPPHATLVFDVELLKLE	
CSP	MRGSH6GSGRLRPQMLRELQRTNAALRDVRELLRQQVKEITRLKNTVRRSRASGKLN	61
$CE_2$ (TRAP)	$\label{eq:mrgsh} MRGSH_6GSACELAARGD(AT)_4AAC\text{-}C\text{-}LQARGD(AT)_4AVDKPIAASA\text{-}E_2\text{-}LEGSGTGAKLN \ (for \ fluorinated CE_2/F\text{-}TRAP, L \ residues \ are \ replaced \ with \ TFL)$	62





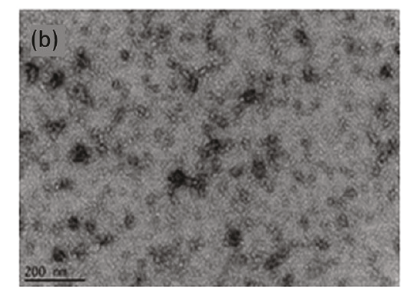
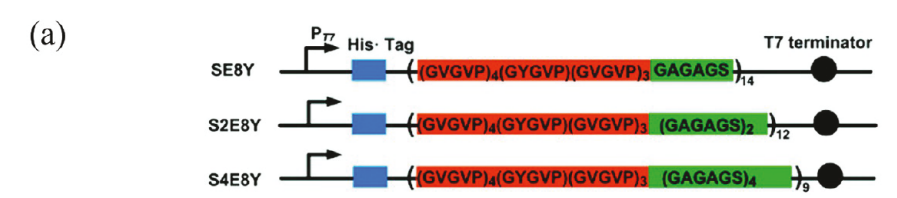


Figure 12. Top panel: Depiction of diblock  $(E_nC \text{ and } C_nE)$  and triblock polymers (ECE and CEC) with their characteristic mechanical properties. TEM images of (a)  $E_1C$  and (b)  $E_1C$  and (c)  $E_1C$  and (d)  $E_1C$  and (e)  $E_1C$  and (e)

tumor site within 10 min of injection that is retained up to 24 h (Figure 16), indicating the ability of such micelles to selectively bind IL-4 receptors with potential use in cancer therapies.<sup>59</sup>

The Mackay group has developed a unique strategy to maximize drug loading and tailor release using an elastin block polymer. Nanoparticles with a hydrophobic core and a hydrophilic corona, referred to as SI, are decorated with FK506 binding protein 12 (FKBP) (Table 2), a protein receptor that binds specifically

to immunosuppressive drugs such as Rapamycin (Rapa). The addition of the FKBP domain to the corona-forming domain of the ELP, did not significantly alter the assembly of the nanoparticles, with the critical micelle temperature (CMT) decreasing from 27 to 24.5 °C and the micelle radius showing a small increase from 15.0  $\pm$  2.3 to 18.5  $\pm$  1.3 nm as depicted by cryo-TEM (Figure 17). Both SI and its FKBP-fused counterpart, referred to as FSI, exhibit high encapsulation efficiency



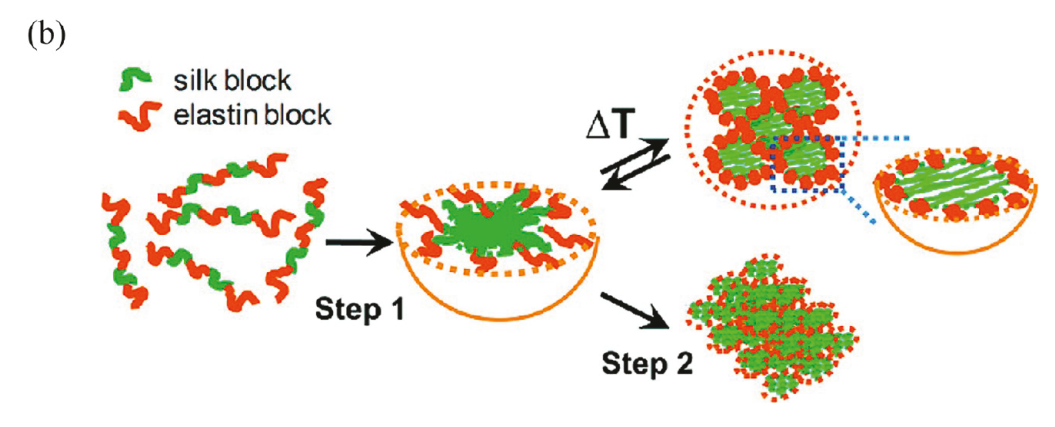


Figure 13. (a) Silk-elastin constructs, SE8Y, S2E8Y, S4E8Y with varying ratios of silk to elastin blocks. (b) Self-assembly of SELPs to form micelle-like particles (step 1). The particles can further coalesce to form larger particles or a gel-like state (step 2). Adapted with permission from ref 48. Copyright 2011 American Chemical Society.

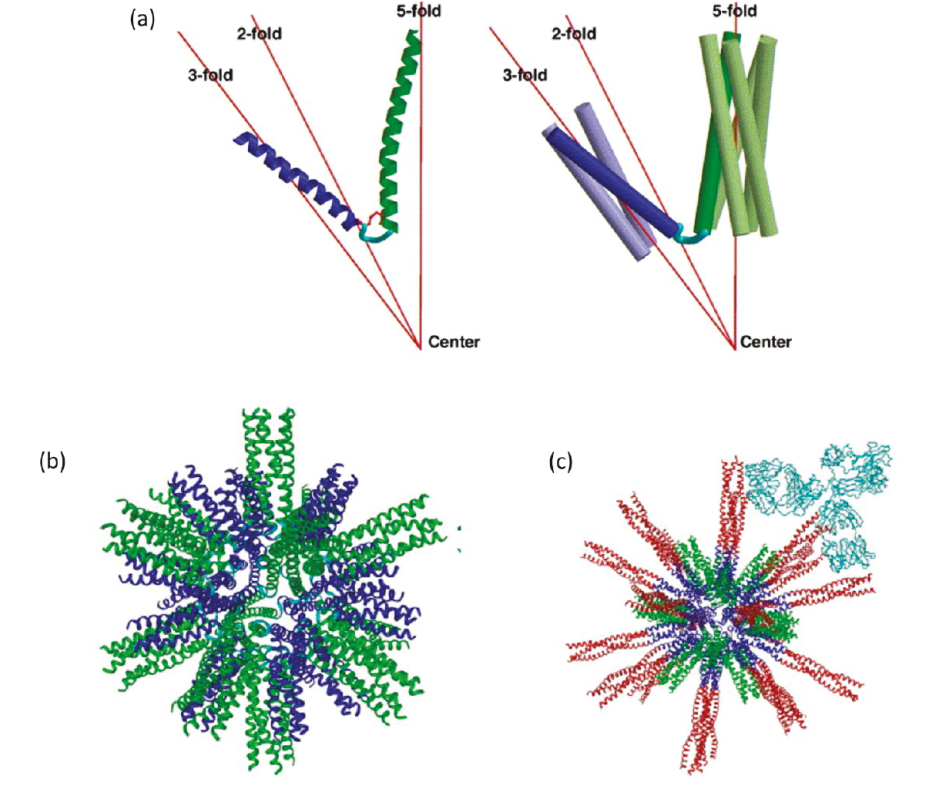
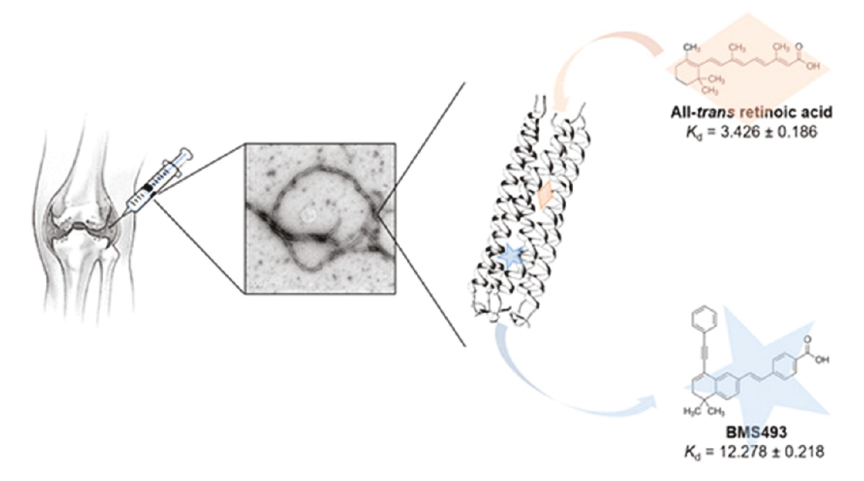


Figure 14. Schematic of self-assembling peptide nanoparticles. (a) Ribbon representation of the monomeric chain comprising of a trimeric coiled-coil (blue) and a pentameric coiled-coil (green) with coiled—coils displayed as cylinders on the right. (b) Computer model of a self-assembled peptide nanoparticle (SAPN). (c) The trimeric coiled-coil of the same nanoparticle was extended by adding the sequence from HIV surface protein gp41 (red), which can be recognized by an antibody (cyan). Adapted with permission from ref 54. Copyright 2006 Elsevier.

of 75% (Figure 17b). FSI nanoparticles present a two-phase release profile comprising of an initial exponential phase with half-life of 1.9 h and a second exponential release with a

half-life of 57.8 h (Figure 17c). On the other hand, SI shows only a single exponential decay with a half-life of 2.2 h. While the initial release is attributed to Rapa binding to the core of



**Figure 15.** Schematic representation of COMPcc<sup>s</sup> nanofibers for drug delivery of BMS-493 in OA joints. Reproduced with permission from ref 24. Copyright 2018 American Chemical Society.

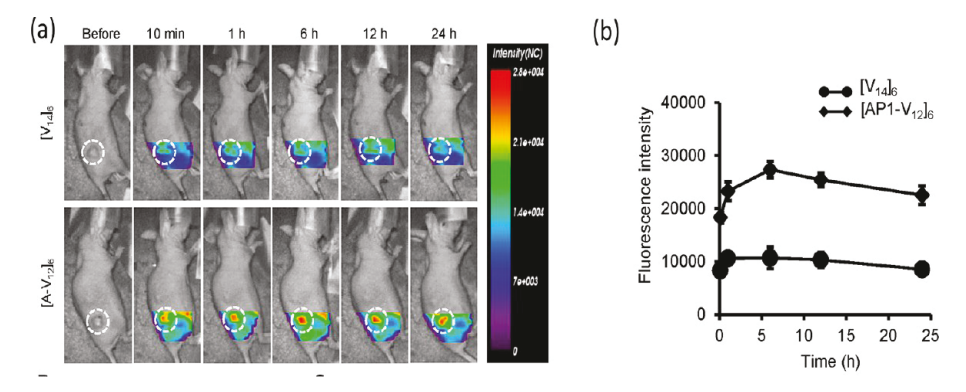


Figure 16. In vivo imaging of  $[V_{14}]_6$  and  $[AP1-V_{12}]_6$  polymers. (a) Fluorophore labeled  $[V_{14}]_6$  and  $[AP1-V_{12}]_6$  were intravenously injected into MDA-MB-231 tumor xenografted nude mice. In vivo fluorescence images were collected at different time points. Scale bar indicates normalized fluorescence intensity. (B) Quantitation of fluorescence intensities in tumor sites at respective time points. Adapted with permission from ref 59. Copyright 2013 Sarangthem, V.; Cho, E. A.; Bae, S. M.; Singh, T. D.; Kim, S. J.; Kim, S. J.; Lee, B. H.; Park, R. W.

the nanoparticles, high-specificity avidity binding of Rapa to the FKBP bearing corona of the micelle contributes to the prolonged release observed for FSI. In addition, FSI-Rapa has been shown to have lower toxicity and better antitumor efficacy than free Rapa in mTOR-dependent breast cancer xenograft mouse model, confirming the utility of such drug-specific carriers. 60

Other block polymers, such as SELPs and CE<sub>2</sub> or thermoresponsive assembled protein (vide infra), have been explored to encapsulate a small chemotherapeutic agent, doxorubicin (Dox) with potential in cancer treatment. S3,62 The micelles composed of SELPs polymers, SE8Y, S2E8Y, S4E8Y (discussed in section 3.1, Table 2), exhibit encapsulation efficiencies varying from 4 to 6.5%. Upon Dox-loading, the micelles of SE8Y, S2E8Y, S4E8Y show an increase in size from  $5.2 \pm 1.8$  nm,  $29 \pm 9.8$  and  $89 \pm 7.3$  nm to  $50 \pm 10$  (SE8Y),  $72 \pm 11$  (S2E8Y), and  $142 \pm 10$  nm (S4E8Y), respectively, at 25 °C. Interestingly, encapsulation of Dox within the silk core drives the self-assembly of micelles into larger particles. At physiological temperature, the average size of the micelles was further increased, in particular for Dox-loaded SE8Y. The Dox-SE8Y micelles also exhibit higher cytotoxicity relative to free Dox and provide a controlled release of the anticancer agent. While the free Dox can freely diffuse through the HeLa cells, Dox-SE8Y micelles (referred as S1/Dox) undergo endocytosis with longer incubation time, facilitating the diffusion of Dox in to the cell nuclei (Figure 18).

Recently, Hill et al. have reported the biosynthesis of a protein block copolymer termed "fluorinated thermoresponsive assembled protein (F-TRAP)", which assembles into monodisperse nanoscaled micelles. 62 The design of the block polymer integrates the coiled-coil domain of cartilage oligomeric matrix protein (C) with two repeats of elastin (E) motif (Table 2). These polymers arrange themselves such that the coiled-coil pentameric units form the corona while the hydrophobic, thermoresponsive E domains sequester to form the core of the micelles. The particle size of these micelles demonstrates a temperature dependent increase. With a rise in temperature from 20 to 50 °C, the particle size increases from  $30.30 \pm 0.60$  to  $952.06 \pm 300.17$  nm.<sup>62</sup> These micelles are capable of encapsulating Dox and releasing its cargo in a thermoresponsive manner. Functionalization of these micelles with trifluoroleucine (TFL), a noncanonical amino acid (NCAA), enables their detection via 19F magnetic resonance imaging (MRI) and <sup>19</sup>F magnetic resonance spectroscopy (MRS) (Figure 19). Successful in vivo <sup>19</sup>F MRI/MRS studies and in vitro Dox delivery encourage the use of F-TRAP micelles as potential diagnostic and therapeutic (theranostic) agents.62

There are several other ways to expand on the potential of protein-based assemblies by using them in combination with metal ions or lipid nanoparticles to obtain hybrid materials of different shapes, sizes, and structures. <sup>6,66,74</sup> Dai et al. have

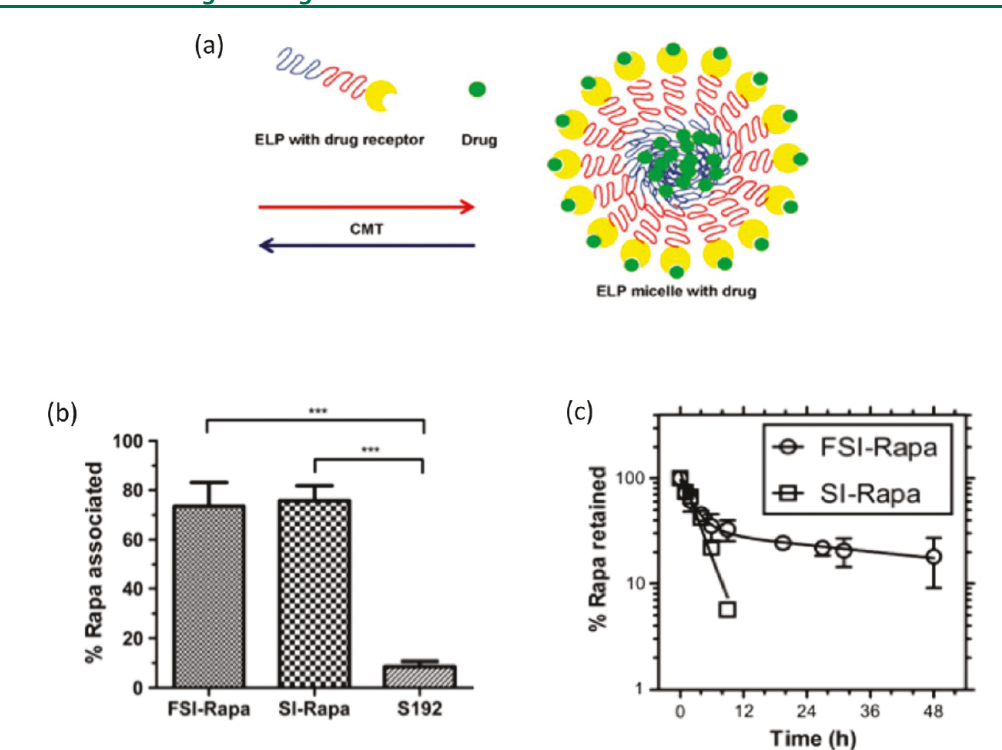
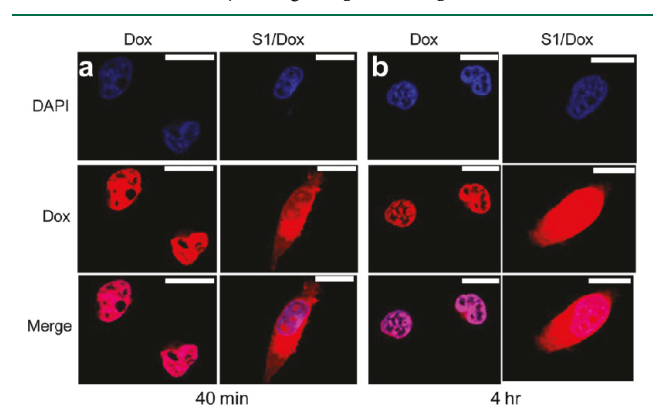
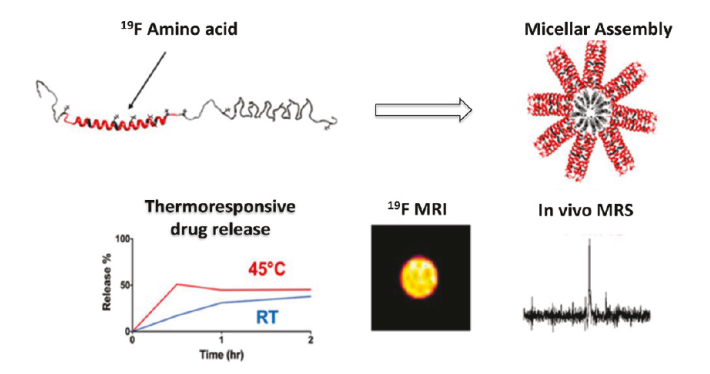


Figure 17. (a) Schematic of ELP micelles capable of binding to the drug (Rapa) both within the core and the FKBP domain of the corona. (b) Both SI and FSI exhibit an encapsulation efficiency of 75%. (c) FSI exhibits two-phase exponential release profile (half-life of 1.9 and 57.8 h), whereas SI exhibits only a single exponential profile half-life of 2.2 h. Adapted with permission from ref 60. Copyright 2013 Elsevier.



**Figure 18.** Confocal laser scanning images of HeLa cells treated with free Dox and Dox-SE8Y micelles (referred as S1/Dox) at (a) 40 min and (b) 4 h. The cell nuclei are stained with DAPI (blue) stain. Scale bar represents 10  $\mu$ m. Adapted with permission from ref 53. Copyright 2014 American Chemical Society.

employed the N-terminal hexahistidine tag of  $CE_1$  and  $E_1C$  (two of the block polymers discussed in section 3.1, Table 2) to template synthesis of gold nanoparticles (AuNPs) resulting in protein-AuNP composites. TEM analysis reveals that these  $CE_1$ -AuNP and  $E_1C$ -AuNP nanocomposites have a particle size of  $\sim\!23$  nm. Furthermore, both  $CE_1$ -AuNP and  $E_1C$ -AuNP exhibit enhanced delivery of curcumin with a 2-fold curcumin uptake in MCF-7 breast cancer cells relative to protein alone (Figure 20). Another approach to design hybrid functional materials entails the use of lipid vesicles called liposomes. These designed lipid-protein complexes, or lipoproteoplexes, have been successfully used for gene and drug delivery. Recently, Montclare and colleagues have proved the utility of such assemblies in which lipofectamine 2000 (L2000) is combined with a supercharged protein for cellular delivery of



**Figure 19.** Schematic illustration of self-assembled micellar structures of F-TRAP. The micelles are capable of thermoresponsive drug release and are detected via <sup>19</sup>F MRI and MRS. Adapted with permission from ref 62. Copyright 2019 American Chemical Society.

Dox with a short interfering RNA (siRNA) (Figure 21a).<sup>76</sup> The supercharged protein (CSP) is a variant of COMPcc, where solvent exposed residues are mutated to arginine (R) that renders a positively charged surface (Table 2). This positive charge allows CSP to bind negatively charged nucleic acids such as DNA and RNA.<sup>61</sup> In a separate study, the lipoproteoplexes that contain siRNA-targeting Keap1, have been effective in accelerating wound healing in mice. The wounds treated with the lipoproteoplex are healed within 22 days, whereas the untreated wounds are healed within 32 days (Figure 21b), confirming not only the successful delivery of siKeap1 but also its efficiency in knocking down Keap1.<sup>77</sup>

### 5. CONCLUSIONS AND PERSPECTIVES

Protein- and peptide-based copolymers are extensively studied for their versatility and propensity to self-assemble into a

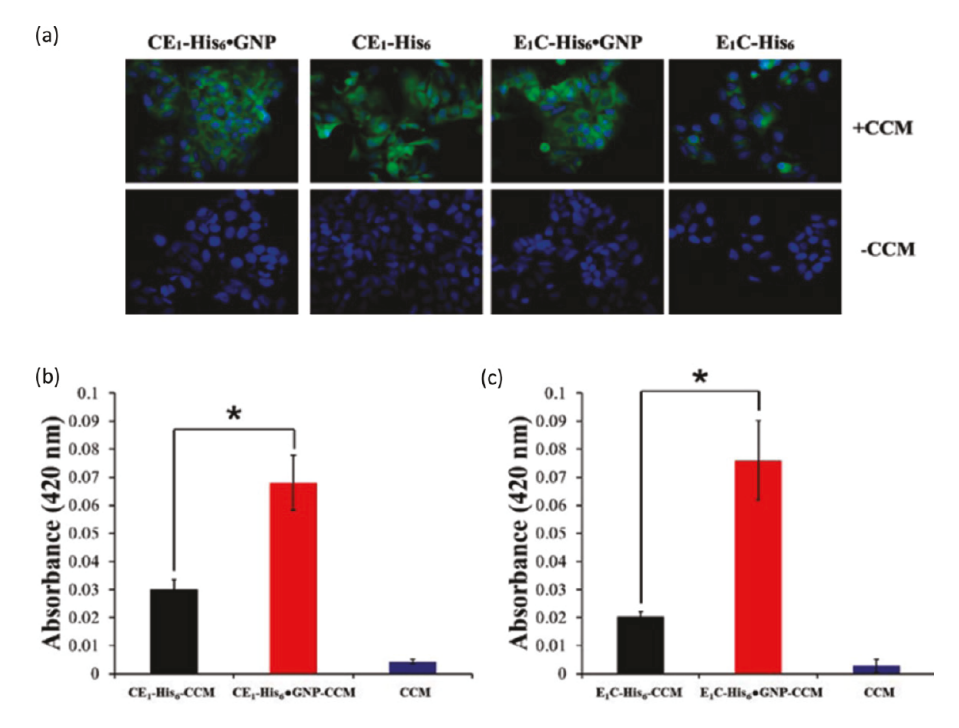


Figure 20. (a) Fluorescence microscopy images of MCF-7 cells that show cellular uptake of curcumin (CCM) with protein block polymers alone or in the presence of protein-AuNP. Extraction of curcumin from the cells reveal enhanced uptake in the presence of (b)  $CE_1$ -AuNP and (c)  $E_1C$ -AuNP, respectively, relative to the block polymers alone. Adapted with permission from ref 75. Copyright 2016 Dai, M.; Frezzo, J. A.; Sharma, E.; Chen, R.; Singh, N.; Yuvienco, C.; Caglar, E.; Xiao, S.; Saxena, A.; Montclare, J. K.

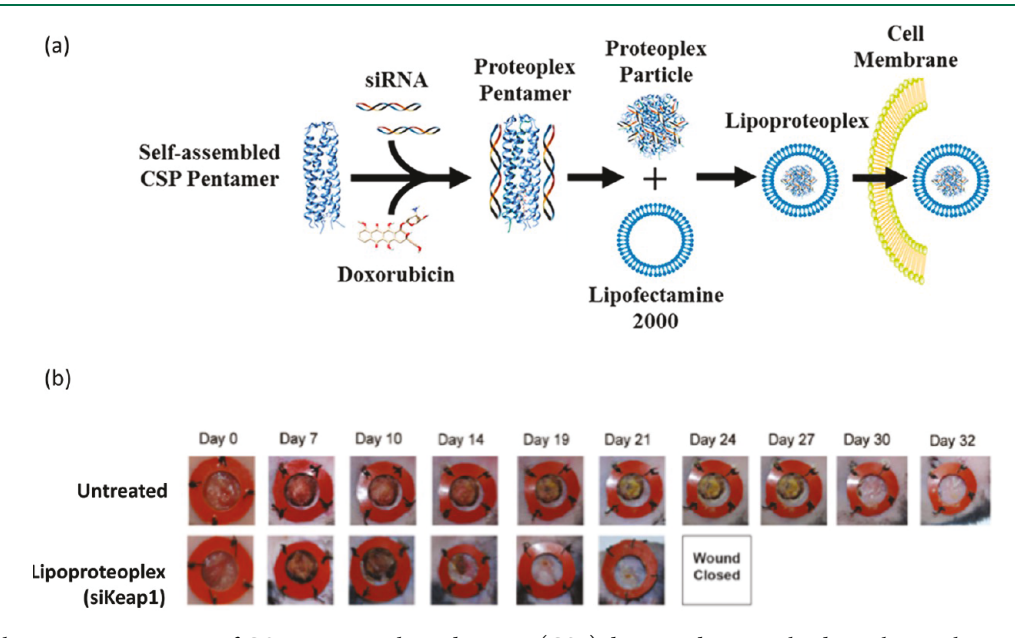


Figure 21. (a) Schematic representation of COMPcc supercharged protein (CSP) design and cationic lipids resulting in lipoproteoplexes for gene (siRNA), drug (doxorubicin), or codelivery. (b) siKeap1 delivery accelerates diabetic wound closure; compared to untreated mice wounds (shown in upper panel), treatment with lipoproteoplexes comprising of DOTAP:sodium cholate and siKeap1 bound to CSP, lessen wound burden in diabetic mice (lower panel). Panel a reproduced with permission from ref 76. Copyright 2017 American Chemical Society. Panel b adapted with permission from ref 77. Copyright 2017 Elsevier.

variety of structures.<sup>2</sup> Although there are no clear design principles that can predict the final morphology of the nanostructures, multiple factors can dictate the assembly into either micelles or nanofibers, among other supramolecular structures. Micelles typically assemble through structural collapse, whereas fibrous materials are designed such that interactions are more ordered. As discussed in the aforementioned examples, the nature of hydrophobic and hydrophilic blocks governs the self-assembly

of protein polymers into particles and fibers of various shapes and sizes. In particular, the length and orientation of the blocks,  $T_{\rm t}$  of the protein polymer, secondary structure elements, and inclusion of non-protein/peptide components can influence the design of these assemblies. Although these trends are often seen, it is important to note that these guidelines are still being developed, with multiple exceptions being observed. In certain cases, modifying the amine- and/or carboxy-termini of proteins

can tune the self-assembly of protein polymers into specific nanoarchitectures.  $^{31,78,79}$  Interestingly, the same protein building blocks can form both micellar and fibrous structures and vice versa, with external stimuli influencing the overall architecture of these assemblies. Several factors ranging from concentration, ionic strength, buffer composition, pH, and even the physicochemical properties of the substrate surface can control the self-assembling properties. For example, Hwang et al. found that SELP415K self-assemble into nanofibers at concentrations above 1  $\mu \rm g \ mL^{-1}$  but form spherical particles when diluted to 0.2  $\mu \rm g \ mL^{-1}$  The SELP polymer also shows a transition from fibers to spherical nanostructures with an increasing ionic strength.  $^{81}$ 

Here, we have provided an overview of two different selfassembled structures for applications in drug as well as gene delivery. Both nanostructures have great potential in encapsulating drugs, cell targeting and biomedical imaging.<sup>8,64</sup> Fibers have high surface to volume ratio offering greater drug loading capacity and ease of surface modification. Micelles, on the other hand, aid in solubilization of hydrophobic drugs that can be sequestered within their core, thereby facilitating the cellular uptake of lipophilic molecules. While there are several advantages of using protein-based micelles and fibers for drug delivery purposes, their in vivo use is limited because of rapid clearance. 4,83 Moreover, degradation by various proteases present within the body can alter the drug release profile leading to inconsistent drug release and biodistribution.83 Other factors such as low protein yield, increased protein production and storage cost, and the need for endotoxin removal impact the development of protein-based formulations.

Despite the challenges, there are plenty of opportunities for developing an ideal protein-engineered system for various biomedical applications. Recent trends toward the development of smart biomaterials have highlighted the importance of hydrogels with applications in tissue engineering and regeneration, targeted drug delivery, gene therapy and bioelectronics. 84-87 Fibers and nanoparticles are each capable of generating higher-order assemblies that can pack together via physical and chemical interactions to form gels and thin films.<sup>88</sup> The incorporation of NCAAs within proteins open exciting and new avenues for generating nanomaterials that are based on the use of monomers that extend beyond the 20 canonical amino acids. 89,90 In addition, the use of protein composite materials is rapidly expanding and have been shown to imbue new functionalities. 91 Furthermore, virus like particles, an emerging class of protein-based nanocarriers, is fast gaining traction and offer several advantages over existing delivery carriers. 92 Overall, protein- and peptide-based assemblies offer promising opportunities in building next-generation smart biomaterials.

### AUTHOR INFORMATION

### **Corresponding Author**

\*Email: montclare@nyu.edu (J.K.M.).

ORCID ®

Jin K. Montclare: 0000-0001-6857-3591

Notes

The authors declare no competing financial interest.

### ACKNOWLEDGMENTS

This work was supported by NSF-DMREF under Award DMR 1728858, NSF-MRSEC Program under Award Number DMR

1420073, NSF BMAT under Award DMR 1505214, ARO W911NF-19-2-0160 and ARO W911NF-19-1-0150, the NYU Shiffrin-Myers Breast Cancer Discovery Fund, the W81XWH-16-1-0483, and the NYU CTSA Grant UL1 TR000038 from the National Center for Advancing Translational Sciences, National Institutes of Health.

### REFERENCES

- (1) Luo, Q.; Hou, C.; Bai, Y.; Wang, R.; Liu, J. Protein Assembly: Versatile Approaches to Construct Highly Ordered Nanostructures. *Chem. Rev.* **2016**, *116* (22), 13571–13632.
- (2) Matsuurua, K. Rational design of self-assembled proteins and peptides for nano- and micro-sized architectures. RSC Adv. 2014, 4 (6), 2942–2953.
- (3) Herrera Estrada, L. P.; Champion, J. A. Protein nanoparticles for therapeutic protein delivery. *Biomater. Sci.* **2015**, 3 (6), 787–99.
- (4) Jain, A.; Singh, S. K.; Arya, S. K.; Kundu, S. C.; Kapoor, S. Protein Nanoparticles: Promising Platforms for Drug Delivery Applications. *ACS Biomater. Sci. Eng.* **2018**, *4* (12), 3939–3961.
- (5) Doncom, K. E. B.; Blackman, L. D.; Wright, D. B.; Gibson, M. I.; O'Reilly, R. K. Dispersity effects in polymer self-assemblies: a matter of hierarchical control. *Chem. Soc. Rev.* **2017**, *46* (14), 4119–4134.
- (6) Freeman, A. Protein-Mediated Biotemplating on the Nanoscale. *Biomimetics* **2017**, 2 (3), 14.
- (7) Mikhalevich, V.; Craciun, I.; Kyropoulou, M.; Palivan, C. G.; Meier, W. Amphiphilic Peptide Self-Assembly: Expansion to Hybrid Materials. *Biomacromolecules* **2017**, *18* (11), 3471–3480.
- (8) Doll, T. A.; Raman, S.; Dey, R.; Burkhard, P. Nanoscale assemblies and their biomedical applications. *J. R. Soc., Interface* **2013**, *10* (80), 20120740.
- (9) Desai, M. S.; Lee, S. W. Protein-based functional nanomaterial design for bioengineering applications. *Wiley Interdiscip Rev. Nanomed Nanobiotechnol* **2015**, 7 (1), 69–97.
- (10) Ulijn, R. V.; Smith, A. M. Designing peptide based nanomaterials. *Chem. Soc. Rev.* **2008**, 37 (4), 664–75.
- (11) Mart, R. J.; Osborne, R. D.; Stevens, M. M.; Ulijn, R. V. Peptide-based stimuli-responsive biomaterials. *Soft Matter* **2006**, 2 (10), 822–835.
- (12) Sharifi, F.; Sooriyarachchi, A. C.; Altural, H.; Montazami, R.; Rylander, M. N.; Hashemi, N. Fiber Based Approaches as Medicine Delivery Systems. *ACS Biomater. Sci. Eng.* **2016**, *2* (9), 1411–1431.
- (13) Woolfson, D. N.; Ryadnov, M. G. Peptide-based fibrous biomaterials: Some things old, new and borrowed. *Curr. Opin. Chem. Biol.* **2006**, *10* (6), 559–67.
- (14) Pawelec, K. M.; Best, S. M.; Cameron, R. E. Collagen: a network for regenerative medicine. *J. Mater. Chem. B* **2016**, 4 (40), 6484–6496.
- (15) Kotch, F. W.; Raines, R. T. Self-assembly of synthetic collagen triple helices. *Proc. Natl. Acad. Sci. U. S. A.* **2006**, 103 (9), 3028–33.
- (16) Kojima, S.; Kuriki, Y.; Yoshida, T.; Yazaki, K.; Miura, K.-i. Fibril Formation by an Amphipathic & alpha;-Helix-Forming Polypeptide Produced by Gene Engineering. *Proc. Jpn. Acad., Ser. B* **1997**, 73 (1), 7–11
- (17) Kojima, S.; Kuriki, Y.; Yazaki, K.; Miura, K. Stabilization of the fibrous structure of an alpha-helix-forming peptide by sequence reversal. *Biochem. Biophys. Res. Commun.* **2005**, 331 (2), 577–82.
- (18) Pandya, M. J.; Spooner, G. M.; Sunde, M.; Thorpe, J. R.; Rodger, A.; Woolfson, D. N. Sticky-end assembly of a designed peptide fiber provides insight into protein fibrillogenesis. *Biochemistry* **2000**, *39* (30), 8728–34.
- (19) Papapostolou, D.; Smith, A. M.; Atkins, E. D.; Oliver, S. J.; Ryadnov, M. G.; Serpell, L. C.; Woolfson, D. N. Engineering nanoscale order into a designed protein fiber. *Proc. Natl. Acad. Sci. U. S. A.* **2007**, *104* (26), 10853–8.
- (20) Malashkevich, V. N.; Kammerer, R. A.; Efimov, V. P.; Schulthess, T.; Engel, J. The crystal structure of a five-stranded coiled coil in COMP: a prototype ion channel? *Science* **1996**, *274* (5288), 761–5.

- (21) Gunasekar, S. K.; Asnani, M.; Limbad, C.; Haghpanah, J. S.; Hom, W.; Barra, H.; Nanda, S.; Lu, M.; Montclare, J. K. N-Terminal Aliphatic Residues Dictate the Structure, Stability, Assembly, and Small Molecule Binding of the Coiled-Coil Region of Cartilage Oligomeric Matrix Protein. *Biochemistry* 2009, 48 (36), 8559–8567.
- (22) Guo, Y.; Bozic, D.; Malashkevich, V. N.; Kammerer, R. A.; Schulthess, T.; Engel, J. All-trans retinol, vitamin D and other hydrophobic compounds bind in the axial pore of the five-stranded coiled-coil domain of cartilage oligomeric matrix protein. *EMBO J.* **1998**, *17* (18), 5265–72.
- (23) Gunasekar, S. K.; Anjia, L.; Matsui, H.; Montclare, J. K. Effects of Divalent Metals on Nanoscopic Fiber Formation and Small Molecule Recognition of Helical Proteins. *Adv. Funct. Mater.* **2012**, 22 (10), 2154–2159.
- (24) Yin, L.; Agustinus, A. S.; Yuvienco, C.; Minashima, T.; Schnabel, N. L.; Kirsch, T.; Montclare, J. K. Engineered Coiled-Coil Protein for Delivery of Inverse Agonist for Osteoarthritis. *Biomacromolecules* **2018**, *19* (5), 1614–1624.
- (25) Ogihara, N. L.; Ghirlanda, G.; Bryson, J. W.; Gingery, M.; DeGrado, W. F.; Eisenberg, D. Design of three-dimensional domain-swapped dimers and fibrous oligomers. *Proc. Natl. Acad. Sci. U. S. A.* **2001**, 98 (4), 1404–9.
- (26) Bennett, M. J.; Schlunegger, M. P.; Eisenberg, D. 3D domain swapping: a mechanism for oligomer assembly. *Protein Sci.* **1995**, 4 (12), 2455–68.
- (27) Hume, J.; Sun, J.; Jacquet, R.; Renfrew, P. D.; Martin, J. A.; Bonneau, R.; Gilchrist, M. L.; Montclare, J. K. Engineered coiled-coil protein microfibers. *Biomacromolecules* **2014**, *15* (10), 3503–10.
- (28) Burgess, N. C.; Sharp, T. H.; Thomas, F.; Wood, C. W.; Thomson, A. R.; Zaccai, N. R.; Brady, R. L.; Serpell, L. C.; Woolfson, D. N. Modular Design of Self-Assembling Peptide-Based Nanotubes. *J. Am. Chem. Soc.* **2015**, *137* (33), 10554–62.
- (29) Reches, M.; Gazit, E. Casting metal nanowires within discrete self-assembled peptide nanotubes. *Science* **2003**, *300* (5619), 625–7.
- (30) Silva, R. F.; Araujo, D. R.; Silva, E. R.; Ando, R. A.; Alves, W. A. L-diphenylalanine microtubes as a potential drug-delivery system: characterization, release kinetics, and cytotoxicity. *Langmuir* **2013**, 29 (32), 10205–12.
- (31) Reches, M.; Gazit, E. Self-assembly of peptide nanotubes and amyloid-like structures by charged-termini-capped diphenylalanine peptide analogues. *Isr. J. Chem.* **2005**, *45* (3), 363–371.
- (32) Liu, J.; Liu, J.; Chu, L.; Zhang, Y.; Xu, H.; Kong, D.; Yang, Z.; Yang, C.; Ding, D. Self-assembling peptide of D-amino acids boosts selectivity and antitumor efficacy of 10-hydroxycamptothecin. ACS Appl. Mater. Interfaces 2014, 6 (8), 5558–65.
- (33) Bella, J.; Eaton, M.; Brodsky, B.; Berman, H. M. Crystal and molecular structure of a collagen-like peptide at 1.9 A resolution. *Science* **1994**, 266 (5182), 75–81.
- (34) Cejas, M. A.; Kinney, W. A.; Chen, C.; Leo, G. C.; Tounge, B. A.; Vinter, J. G.; Joshi, P. P.; Maryanoff, B. E. Collagen-related peptides: self-assembly of short, single strands into a functional biomaterial of micrometer scale. *J. Am. Chem. Soc.* **2007**, *129* (8), 2202–3.
- (35) Cejas, M. A.; Kinney, W. A.; Chen, C.; Vinter, J. G.; Almond, H. R., Jr.; Balss, K. M.; Maryanoff, C. A.; Schmidt, U.; Breslav, M.; Mahan, A.; Lacy, E.; Maryanoff, B. E. Thrombogenic collagenmimetic peptides: Self-assembly of triple helix-based fibrils driven by hydrophobic interactions. *Proc. Natl. Acad. Sci. U. S. A.* **2008**, *105* (25), 8513–8.
- (36) Paramonov, S. E.; Gauba, V.; Hartgerink, J. D. Synthesis of Collagen-like Peptide Polymers by Native Chemical Ligation. *Macromolecules* **2005**, 38 (18), 7555–7561.
- (37) Rele, S.; Song, Y.; Apkarian, R. P.; Qu, Z.; Conticello, V. P.; Chaikof, E. L. D-periodic collagen-mimetic microfibers. *J. Am. Chem. Soc.* **2007**, *129* (47), 14780–7.
- (38) O'Leary, L. E.; Fallas, J. A.; Bakota, E. L.; Kang, M. K.; Hartgerink, J. D. Multi-hierarchical self-assembly of a collagen mimetic peptide from triple helix to nanofibre and hydrogel. *Nat. Chem.* **2011**, 3 (10), 821–8.

- (39) Lopez-Silva, T. L.; Leach, D. G.; Li, I. C.; Wang, X.; Hartgerink, J. D. Self-Assembling Multidomain Peptides: Design and Characterization of Neutral Peptide-Based Materials with pH and Ionic Strength Independent Self-Assembly. ACS Biomater. Sci. Eng. 2019, 5 (2), 977–985.
- (40) Cappello, J. Protein engineering for biomaterials applications. *Curr. Opin. Struct. Biol.* **1992**, *2* (4), 582–586.
- (41) Rabotyagova, O. S.; Cebe, P.; Kaplan, D. L. Protein-based block copolymers. *Biomacromolecules* **2011**, *12* (2), 269–89.
- (42) Wright, E. R.; Conticello, V. P. Self-assembly of block copolymers derived from elastin-mimetic polypeptide sequences. *Adv. Drug Delivery Rev.* **2002**, *54* (8), 1057–73.
- (43) Urry, D. W. Free energy transduction in polypeptides and proteins based on inverse temperature transitions. *Prog. Biophys. Mol. Biol.* **1992**, *57* (1), 23–57.
- (44) MacEwan, S. R.; Chilkoti, A. Elastin-like polypeptides: Biomedical applications of tunable biopolymers. *Biopolymers* **2010**, 94 (1), 60–77.
- (45) Urry, D. W. Physical Chemistry of Biological Free Energy Transduction As Demonstrated by Elastic Protein-Based Polymers. *J. Phys. Chem. B* **1997**, *101* (51), 11007–11028.
- (46) Dreher, M. R.; Simnick, A. J.; Fischer, K.; Smith, R. J.; Patel, A.; Schmidt, M.; Chilkoti, A. Temperature triggered self-assembly of polypeptides into multivalent spherical micelles. *J. Am. Chem. Soc.* **2008**, *130* (2), *687*–94.
- (47) Luo, T.; Kiick, K. L. Noncovalent Modulation of the Inverse Temperature Transition and Self-Assembly of Elastin-b-Collagen-like Peptide Bioconjugates. *J. Am. Chem. Soc.* **2015**, *137* (49), 15362–5.
- (48) Xia, X. X.; Xu, Q.; Hu, X.; Qin, G.; Kaplan, D. L. Tunable self-assembly of genetically engineered silk-elastin-like protein polymers. *Biomacromolecules* **2011**, *12* (11), 3844–50.
- (49) Dai, M.; Haghpanah, J.; Singh, N.; Roth, E. W.; Liang, A.; Tu, R. S.; Montclare, J. K. Artificial protein block polymer libraries bearing two SADs: effects of elastin domain repeats. *Biomacromolecules* **2011**, 12 (12), 4240–6.
- (50) Haghpanah, J. S.; Yuvienco, C.; Civay, D. E.; Barra, H.; Baker, P. J.; Khapli, S.; Voloshchuk, N.; Gunasekar, S. K.; Muthukumar, M.; Montclare, J. K. Artificial protein block copolymers blocks comprising two distinct self-assembling domains. *ChemBioChem* **2009**, *10* (17), 2733–5.
- (51) Haghpanah, J. S.; Yuvienco, C.; Roth, E. W.; Liang, A.; Tu, R. S.; Montclare, J. K. Supramolecular assembly and small molecule recognition by genetically engineered protein block polymers composed of two SADs. *Mol. BioSyst.* **2010**, *6* (9), 1662–7.
- (52) Olsen, A. J.; Katyal, P.; Haghpanah, J. S.; Kubilius, M. B.; Li, R.; Schnabel, N. L.; O'Neill, S. C.; Wang, Y.; Dai, M.; Singh, N.; Tu, R. S.; Montclare, J. K. Protein Engineered Triblock Polymers Composed of Two SADs: Enhanced Mechanical Properties and Binding Abilities. *Biomacromolecules* **2018**, *19* (5), 1552–1561.
- (53) Xia, X. X.; Wang, M.; Lin, Y.; Xu, Q.; Kaplan, D. L. Hydrophobic drug-triggered self-assembly of nanoparticles from silk-elastin-like protein polymers for drug delivery. *Biomacromolecules* **2014**, *15* (3), 908–14.
- (54) Raman, S.; Machaidze, G.; Lustig, A.; Aebi, U.; Burkhard, P. Structure-based design of peptides that self-assemble into regular polyhedral nanoparticles. *Nanomedicine* **2006**, 2 (2), 95–102.
- (55) Indelicato, G.; Wahome, N.; Ringler, P.; Muller, S. A.; Nieh, M. P.; Burkhard, P.; Twarock, R. Principles Governing the Self-Assembly of Coiled-Coil Protein Nanoparticles. *Biophys. J.* **2016**, *110* (3), 646–660
- (56) Burkhard, P.; Lanar, D. E. Malaria vaccine based on self-assembling protein nanoparticles. *Expert Rev. Vaccines* **2015**, *14* (12), 1525–7.
- (57) Karch, C. P.; Li, J.; Kulangara, C.; Paulillo, S. M.; Raman, S. K.; Emadi, S.; Tan, A.; Helal, Z. H.; Fan, Q.; Khan, M. I.; Burkhard, P. Vaccination with self-adjuvanted protein nanoparticles provides protection against lethal influenza challenge. *Nanomedicine* **2017**, *13* (1), 241–251.

- (58) Pimentel, T. A.; Yan, Z.; Jeffers, S. A.; Holmes, K. V.; Hodges, R. S.; Burkhard, P. Peptide nanoparticles as novel immunogens: design and analysis of a prototypic severe acute respiratory syndrome vaccine. *Chem. Biol. Drug Des.* **2009**, *73* (1), 53–61.
- (59) Sarangthem, V.; Cho, E. A.; Bae, S. M.; Singh, T. D.; Kim, S. J.; Kim, S.; Jeon, W. B.; Lee, B. H.; Park, R. W. Construction and application of elastin like polypeptide containing IL-4 receptor targeting peptide. *PLoS One* **2013**, *8* (12), e81891.
- (60) Shi, P.; Aluri, S.; Lin, Y. A.; Shah, M.; Edman, M.; Dhandhukia, J.; Cui, H.; MacKay, J. A. Elastin-based protein polymer nanoparticles carrying drug at both corona and core suppress tumor growth in vivo. *J. Controlled Release* **2013**, *171* (3), 330–8.
- (61) More, H. T.; Frezzo, J. A.; Dai, J.; Yamano, S.; Montclare, J. K. Gene delivery from supercharged coiled-coil protein and cationic lipid hybrid complex. *Biomaterials* **2014**, *35* (25), 7188–93.
- (62) Hill, L. K.; Frezzo, J. A.; Katyal, P.; Hoang, D. M.; Ben Youss Gironda, Z.; Xu, C.; Xie, X.; Delgado-Fukushima, E.; Wadghiri, Y. Z.; Montclare, J. K. Protein-Engineered Nanoscale Micelles for Dynamic (19)F Magnetic Resonance and Therapeutic Drug Delivery. ACS Nano 2019, 13, 2969.
- (63) Gagner, J. E.; Kim, W.; Chaikof, E. L. Designing protein-based biomaterials for medical applications. *Acta Biomater.* **2014**, *10* (4), 1542–57.
- (64) Yin, L.; Yuvienco, C.; Montclare, J. K. Protein based therapeutic delivery agents: Contemporary developments and challenges. *Biomaterials* **2017**, *134*, 91–116.
- (65) Maham, A.; Tang, Z.; Wu, H.; Wang, J.; Lin, Y. Protein-based nanomedicine platforms for drug delivery. *Small* **2009**, 5 (15), 1706–21.
- (66) Katyal, P.; Montclare, J. K. Design and Characterization of Fibers and Bionanocomposites Using the Coiled-Coil Domain of Cartilage Oligomeric Matrix Protein. *Methods Mol. Biol.* **2018**, *1798*, 239–263.
- (67) Frezzo, J. A.; Montclare, J. K. Exploring the potential of engineered coiled-coil protein microfibers in drug delivery. *Ther. Delivery* **2015**, *6* (6), 643–646.
- (68) Floss, D. M.; Schallau, K.; Rose-John, S.; Conrad, U.; Scheller, J. Elastin-like polypeptides revolutionize recombinant protein expression and their biomedical application. *Trends Biotechnol.* **2010**, 28 (1), 37–45.
- (69) MacEwan, S. R.; Chilkoti, A. Applications of elastin-like polypeptides in drug delivery. J. Controlled Release 2014, 190, 314–30.
- (70) Urry, D. W.; Pattanaik, A.; Jie, X.; Cooper Woods, T.; McPherson, D. T.; Parker, T. M. Elastic protein-based polymers in soft tissue augmentation and generation. *J. Biomater. Sci., Polym. Ed.* **1998**, 9 (10), 1015–1048.
- (71) Baker, P. J.; Haghpanah, J. S.; Montclare, J. K., Elastin-Based Protein Polymers. In *Polymer Biocatalysis and Biomaterials II*; American Chemical Society: 2008; Vol. 999, pp 37–51.
- (72) Kim, W.; Xiao, J.; Chaikof, E. L. Recombinant amphiphilic protein micelles for drug delivery. *Langmuir* **2011**, 27 (23), 14329–34
- (73) Rodriguez-Cabello, J. C.; Arias, F. J.; Rodrigo, M. A.; Girotti, A. Elastin-like polypeptides in drug delivery. *Adv. Drug Delivery Rev.* **2016**, 97, 85–100.
- (74) Girard-Egrot, A.; Blum, L.; Richter, R.; Brisson, A., Protein—Lipid Assembly and Biomimetic Nanostructures. In *Nanoscience: Nanobiotechnology and Nanobiology*; Boisseau, P., Houdy, P., Lahmani, M., Eds.; Springer: Berlin, 2009; pp 29–100.
- (75) Dai, M.; Frezzo, J. A.; Sharma, E.; Chen, R.; Singh, N.; Yuvienco, C.; Caglar, E.; Xiao, S.; Saxena, A.; Montclare, J. K., Engineered Protein Polymer-Gold Nanoparticle Hybrid Materials for Small Molecule Delivery. *J. Nanomed. Nanotechnol.* **2016**, 7 (1), DOI: 10.4172/2157-7439.1000356.
- (76) Liu, C. F.; Chen, R.; Frezzo, J. A.; Katyal, P.; Hill, L. K.; Yin, L.; Srivastava, N.; More, H. T.; Renfrew, P. D.; Bonneau, R.; Montclare, J. K. Efficient Dual siRNA and Drug Delivery Using Engineered Lipoproteoplexes. *Biomacromolecules* **2017**, *18* (9), 2688–2698.

- (77) Rabbani, P. S.; Zhou, A.; Borab, Z. M.; Frezzo, J. A.; Srivastava, N.; More, H. T.; Rifkin, W. J.; David, J. A.; Berens, S. J.; Chen, R.; Hameedi, S.; Junejo, M. H.; Kim, C.; Sartor, R. A.; Liu, C. F.; Saadeh, P. B.; Montclare, J. K.; Ceradini, D. J. Novel lipoproteoplex delivers Keap1 siRNA based gene therapy to accelerate diabetic wound healing. *Biomaterials* **2017**, *132*, 1–15.
- (78) Aluri, S.; Pastuszka, M. K.; Moses, A. S.; MacKay, J. A. Elastin-like peptide amphiphiles form nanofibers with tunable length. *Biomacromolecules* **2012**, *13* (9), 2645–54.
- (79) Yu, Y.-C.; Berndt, P.; Tirrell, M.; Fields, G. B. Self-Assembling Amphiphiles for Construction of Protein Molecular Architecture. *J. Am. Chem. Soc.* **1996**, *118* (50), 12515–12520.
- (80) Beun, L. H.; Storm, I. M.; Werten, M. W.; de Wolf, F. A.; Cohen Stuart, M. A.; de Vries, R. From micelles to fibers: balancing self-assembling and random coiling domains in pH-responsive silk-collagen-like protein-based polymers. *Biomacromolecules* **2014**, *15* (9), 3349–57
- (81) Hwang, W.; Kim, B. H.; Dandu, R.; Cappello, J.; Ghandehari, H.; Seog, J. Surface Induced nanofiber growth by self-assembly of a silk-elastin-like protein polymer. *Langmuir* **2009**, 25 (21), 12682–6.
- (82) Yan, X.; Cui, Y.; He, Q.; Wang, K.; Li, J.; Mu, W.; Wang, B.; Ou-Yang, Z. C. Reversible transitions between peptide nanotubes and vesicle-like structures including theoretical modeling studies. *Chem. Eur. J.* **2008**, *14* (19), 5974–80.
- (83) Frandsen, J. L.; Ghandehari, H. Recombinant protein-based polymers for advanced drug delivery. *Chem. Soc. Rev.* **2012**, *41* (7), 2696–706.
- (84) Jonker, A. M.; Löwik, D. W. P. M.; van Hest, J. C. M. Peptide-and Protein-Based Hydrogels. *Chem. Mater.* **2012**, 24 (5), 759–773.
- (85) Torculas, M.; Medina, J.; Xue, W.; Hu, X. Protein-Based Bioelectronics. ACS Biomater. Sci. Eng. 2016, 2 (8), 1211–1223.
- (86) Haider, M.; Leung, V.; Ferrari, F.; Crissman, J.; Powell, J.; Cappello, J.; Ghandehari, H. Molecular engineering of silk-elastinlike polymers for matrix-mediated gene delivery: biosynthesis and characterization. *Mol. Pharmaceutics* **2005**, 2 (2), 139–50.
- (87) Wang, Y.; Katyal, P.; Montclare, J. K. Protein-Engineered Functional Materials. Adv. Healthcare Mater. 2019, 8 (11), 1801374.
- (88) Dooling, L. J.; Tirrell, D. A., CHAPTER 5 Peptide and Protein Hydrogels. In *Polymeric and Self Assembled Hydrogels: From Fundamental Understanding to Applications*; The Royal Society of Chemistry: 2013; pp 93–124.
- (89) More, H. T.; Zhang, K. S.; Srivastava, N.; Frezzo, J. A.; Montclare, J. K. Influence of fluorination on protein-engineered coiled-coil fibers. *Biomacromolecules* **2015**, *16* (4), 1210–7.
- (90) Yuvienco, C.; More, H. T.; Haghpanah, J. S.; Tu, R. S.; Montclare, J. K. Modulating supramolecular assemblies and mechanical properties of engineered protein materials by fluorinated amino acids. *Biomacromolecules* **2012**, *13* (8), 2273–8.
- (91) Hu, X.; Cebe, P.; Weiss, A. S.; Omenetto, F.; Kaplan, D. L. Protein-based composite materials. *Mater. Today* **2012**, *15* (5), 208–215
- (92) Rohovie, M. J.; Nagasawa, M.; Swartz, J. R. Virus-like particles: Next-generation nanoparticles for targeted therapeutic delivery. *Bioeng Transl Med.* **2017**, 2 (1), 43–57.